Theses and Dissertations Thesis Collection

1966-05

A model study of acoustic reflection from a rippled water-sand interface

Arcuni, Philip W.

http://hdl.handle.net/10945/9583

A MODEL STUDY OF ACOUSTIC REFLECTION FROM
A RIPPLED WATER-SAND INTERFACE

PHILIP ARCUNI

A MODEL STUDY OF ACOUSTIC REFLECTION FROM

A RIPPLED WATER-SAND INTERFACE

by

Philip Arcuni
Lieutenant Commander, United States Navy
B. S., United States Naval Academy, 1957

Submitted in partial fulfillment
for the degree of

MASTER OF SCIENCE IN ENGINEERING ELECTRONICS

from the

UNITED STATES NAVAL POSTGRADUATE SCHOOL
May 1966

ABSTRACT

A model experiment was performed to measure acoustic reflection from a rippled sand surface using a pulse-echo system employing electro-static transducers over the frequency range 100-350 kHz. The ripple wave-length of 1.23 cm was slightly greater than the longest acoustic wave-length and had an amplitude to wavelength ratio of 1/10. Boiling of the sand to remove entrapped air was essential before the scattering effects of the ripples could be observed. The angles of propagation of the scat-tered spectra are found to agree with the theoretical prediction within $\pm$ 2°. The amplitudes of two orders of the scattered spectrum were mea-sured at an incident angle of 45° and compared to the theory for the limiting condition where the ripple wavelength is very much larger than the acoustic wavelength. Agreement was excellent for the spectral re-flection, but was not as good for the first order reflection.

TABLE OF CONTENTS

3

LIST OF ILLUSTRATIONS

5

6

Table of Symbols

C_1,   speed of sound in fresh water-1480 m/sec.

C_2,   speed of sound in water-saturated sand-1740 m/sec.

ρ_1,   density of fresh water-1.00

ρ_2,   density of water-saturated sand-2.01

w,   radian frequency

r,   distance from transducer

R,   range from transmitter to receiver along spectrally reflected ray path

λ,   acoustic wavelength in water

λ_s,   wavelength of ripples on sand surface

$k = w/C_1 = 2\pi/\lambda$, wave number in water

$p = 2\pi/\lambda_s$, wave number of sand surface ripples

Θ,   angle of incidence (measured from normal)
          $0 \le \Theta \le 90$

Θ_c,   critical angle of incidence

Θ_t,   angle of refracted ray in the reflecting medium (measured from normal)

$\Theta_g = 90° - \Theta$, grazing angle of transmitted energy

$\Theta_m = \cos^{-1} a_m$, grazing angle of mth order scattered wave

$m = 0, 1, 2, ...$

$a_m = \cos \Theta_m$, direction cosine with respect to horizontal of mth order scattered wave $-1 < a_m < +1$

A_m,   amplitude of mth order scattered wave

α_r,   sound pressure reflection coefficient for plane interface

$a_o = \cos \Theta_g$, Direction cosine with respect to horizontal of incident wave

h,   sine wave amplitude of rippled surface; surface = h cos px

7

1. Introduction

The importance of acoustics in searching the oceans for objects such as submarines, mines and fish has long been established, and much, though still not enough, is known about the transmission of sound in the water itself.

In addition, many added problems occur upon consideration of the boundaries of the ocean, since they complicate the situation so drastically. The ocean surface, a near perfect reflecting surface due to the extreme acoustic mismatch, acts as a simple reflector when flat, but is capable of considerable scattering when roughened by wind and waves. Several studies have been made of scattering from random and periodic ocean surface roughness. [3,6,12, 21]

The other ocean boundary, the bottom, is also of great interest, especially when considering the search for mines and other debris on the bottom, as well as the Navy's interest in long range bottom-bounce SONAR. Many studies have been made, both in the laboratory and in-situ, of the acoustic properties of ocean bottom materials with a view toward obtaining possible reflection characteristics of the sediments found in large parts of the oceans. [1,4,5,14,19]

Studies at sea of the effect of the ocean bottom on acoustic propagation are being conducted continually. [13] Certainly much is to be gained from such field studies, and, in the final analysis, all theories must be evaluated at sea if they are to be useful in explaining actual phenomenon. However, experiments at sea are expensive, and, in general, the conditions of the experiments are difficult to control.

If workable techniques can be developed, scale model studies in small laboratory tanks can provide much basic information about various phenomena. In the laboratory all the parameters of the experiment can be carefully examined and controlled, and valuable testing of recent as well as older theories provided at minimum expense. Horton describes several model experiments and builds a good case for scale model studies. [7]

The reflection from a boundary is not only a function of the acoustic properties of the media involved but of the shape of the interface as well. Photographic studies of the ocean bottom indicate that it is far from flat. Of special interest is the existance of nearly periodic, extended, coherent ripples on portions of the deep ocean floor. [18] Nearly everyone has seen ripples on a sandy beach and in shallow water caused by wave action. [2] Those on the deep ocean are caused by steady currents, much as a steady wind causes ripples on desert sand. From an acoustical reflection viewpoint, one of the more interesting characteristics of these ripples is the unusually long wave-lengths. Periodic ripples up to twelve inches apart have been found in 1000 fathoms of water. This is close to the wavelength of many SONARS in use today. It seems apparent that sound waves having a similar wavelength and striking such a surface would be diffracted in much the same way as light striking a diffraction grating.

The study of acoustic reflections from periodic rippled surfaces began with Rayleigh. [11] The many theoretical works through the present time are excellently reviewed, with the salient features of each presented, by Spitznoggle. [20]

Experimental work on this topic is rather scarce. In one such

10

study LaCasce and Tamarkin used a corrugated floating cork boundary and obtained results reasonably consistent with earlier theories so long as the assumption of a small surface slope was adhered to. [9] Many of the theoretical studies made since 1955 depend on this work for comparison with experiment. Spitznoggle mentions briefly some as yet unpublished work with corrugated styrofoam being conducted at Defense Research Laboratory, Austin, Texas.

There is only one study that considers a corrugated boundary other than pressure release. Yen and Middleton used a hardened plaster-sand mixture for the corrugated boundary. [22] The corrugation wavelength was approximately five times that of the acoustic wavelength. Due apparently to noise and use of an omnidirectional receiver, the higher order diffraction spectra are not as clearly defined as those described by Spitznoggle.

The experiments described herein are concerned with reflections from a rippled sand boundary utilizing acoustic wavelengths only slightly larger than the ripple wavelength. This wavelength ratio was selected since it seems to occur in practice, and it is convenient for laboratory study.

There were three objectives for the experiment. First, to develop pulse techniques for the conduct of acoustic model experiments in a small reverberant tank; second, to study the feasibility of combining the use of actual ocean bottom material with a rippled boundary in a model experiment; and third, to compare the results with suitable theory for reflection from periodic surfaces.

2. Theory

The simplest theory for the reflection of acoustic waves from a fluid-fluid interface considers plane waves incident on a plane surface. Extensive theoretical work has been done on spherical waves reflecting from a plane fluid-fluid interface, however, the more difficult problem of reflection from a sinusoidal surface has been studied only for plane waves. Plane waves are not easily obtained in a small tank. As a result, in order to compare experimental results with available theories, it is important to consider the conditions which must be fulfilled to allow plane wave theory to be used.

Officer discusses these conditions for a point source in the vicinity of a plane boundary. [15] This work shows that when

$$\frac{1}{R/\lambda \left[(c_1/c_2)^2 - \sin^2 \Theta \right]^{3/2}} \ll 1$$

the plane wave reflection coefficient may be taken as a valid approximation for the reflection of an incident spherical wave. (See table of symbols)

As long as $(c_1/c_2)^2 - \sin^2 \Theta$ is not zero, a wavelength small compared to the range satisfies this condition. (In this experiment R/λ ranges between 74 and 268). However, if $c_2 > c_1$ as is the case here, and the incident angle approaches too closely to the critical angle $(\sin \Theta_c = c_1/c_2)$, the approximation is no longer valid for a finite value of R/λ .

If the expression "very much less than one" ($\ll$ 1) is taken to be equivalent to "less than one-tenth" (< 0.1), one can solve for the limiting angle for which the approximation remains valid. In the case of the

12

sand-water interface considered here:

$$C_1 = 1.48 \times 10^5 \text{ cm/sec}$$

$$C_2 = 1.74 \times 10^5 \text{ cm/sec}$$

$$R = 109 \text{ cm}$$

$$\lambda = 1.48 \text{ cm}$$

$$\Theta_c = 57°$$

and the limiting angle turns out to be approximately 53 degrees.

For those incident angles less than 53 degrees the Rayleigh re-
flection coefficient for plane waves incident on a plane fluid-fluid
interface can be used. [8]

$$\alpha_r = \frac{\rho_2 C_2 \cos \Theta - \rho_1 C_1 \cos \Theta_t}{\rho_2 C_2 \cos \Theta + \rho_1 C_1 \cos \Theta_t}$$

One incident angle used in the experiment was less than the 53
degree limiting angle described above. Problems at this large angle
can occur due to the arrival at the receiver of energy from the re-
fracted wave in the reflecting medium which re-enters the incident
medium. This refraction arrival, as referred to by Officer, or lateral
wave, as referred to by Landau, takes the form of a conical wave pro-
pagating into the incident medium at an angle equal to the critical
angle Θ_c . [10]

Landau and Officer both obtain solutions for the lateral wave, but
only for long ranges. No evidence that the lateral wave appears signi-
ficantly was obtained during the experiment.

A fluid-fluid interface has been assumed throughout. That the water-
saturated sand does indeed behave as a fluid at wavelengths large com-
pared to particle size has been experimentally shown by Nolle. [14]

13

The majority of theoretical studies of sound scattering from periodic surfaces assume the incident wave is a plane wave. [3,6,11, 21] However, considering the approximations shown above, valid comparisons can be made with experimental results.

These studies differ mainly in their initial approach to the problem, the method of evaluating the coefficients of the resulting series solution, and in the restrictions placed on the parameters of the periodic surface. They vary in complexity from the earliest of Rayleigh, through attempts to improve on Rayleigh, to the theory of Uretsky, which is the least restrictive and the most all encompassing. However, this last theory, as explained by Spitznoggle, involves lengthy and complex numerical methods including inversion of an infinite matrix. [20]

The reflected radiation is composed of a specular reflection as well as the nonspecular scattered orders. The angles at which these scattered spectra are propagated can be determined directly from the wave equation without application of any boundary conditions. Hence, all the theories essentially agree that these angles can be given by: [9]

$$a_m = a_o + mp/k \qquad m = 0, \pm 1, \pm 2, \cdots$$

A great deal of effort has been expended on further solution of the problem. This has entailed, through application of appropriate boundary conditions, determination of the coefficients of the series solution to the wave equation. The terms of this series represent the amplitudes of the various scattered spectra. Rayleigh's work in this area, applicable only when the ripple wavelength (λ_s) is very large compared to the acoustic wavelength (λ), leads to the result:

14

$$A_o = \alpha_r \, J_o \, (2 h k \cos \theta)$$

$$A_m = \alpha_r \, 2(j)^m \, J_m \, (2 k h \cos \theta) \qquad m \neq 0$$

Under the condition where the ripple wavelength is only slightly greater than the acoustic wavelength, Rayleigh solved the problem only when the reflecting surface is of the pressure-release type. All the later studies also deal only with this type of boundary, and as yet, no one has developed a theoretical solution for the general case. Expressions for the scattered spectra amplitudes are somewhat more involved in the pressure-release situation than in those given above, and it can be safely assumed that such would be the case for a general reflecting surface. LaCasce indicates that the amplitudes of the lower order spectra are functions of the higher orders.

3.   Apparatus

Tank

The water tank, 8 feet long, 4 feet wide, and 3 feet deep, was
constructed of one quarter inch steel plate and reinforced by one and
one half inch angle-iron around its upper edge and middle. The bare
steel was cleaned and coated with Sherwin Williams Chemical and Moisture
Resistant Primer and Paint to prevent corrosion. This treatment appear-
ed completely satisfactory for corrosion prevention needing only occasion-
al touch-up where the finish was scratched or physically marred. It was
not judged necessary to provide the tank with acoustic insulation due to
the use of pulse techniques, as reverberation from each pulse could be
allowed to decay completely before the next pulse is transmitted.

Transducer Support

The transducer support (Fig. 3.1) consisted of a large, four foot
by six foot, aluminum and steel frame placed in the bottom of the tank.
Two arms for supporting the sending and receiving transducers were mount-
ed coaxially on a bearing and shaft attached to the frame. The signal
source transducer was mounted on one of the arms at a distance of 72 cm.
from the shaft. This arm could be rotated through 90 degrees from hori-
zontal to vertical positions. The receiving transducer was mounted on
the other arm at a distance of 37 cm. from the shaft. Considerable care
was required to ensure that the transducer faces were carefully aligned
perpendicular to the support arms so that they would always be pointed
at the same portion of the reflecting surface.

The receiving transducer support arm was constructed of light weight
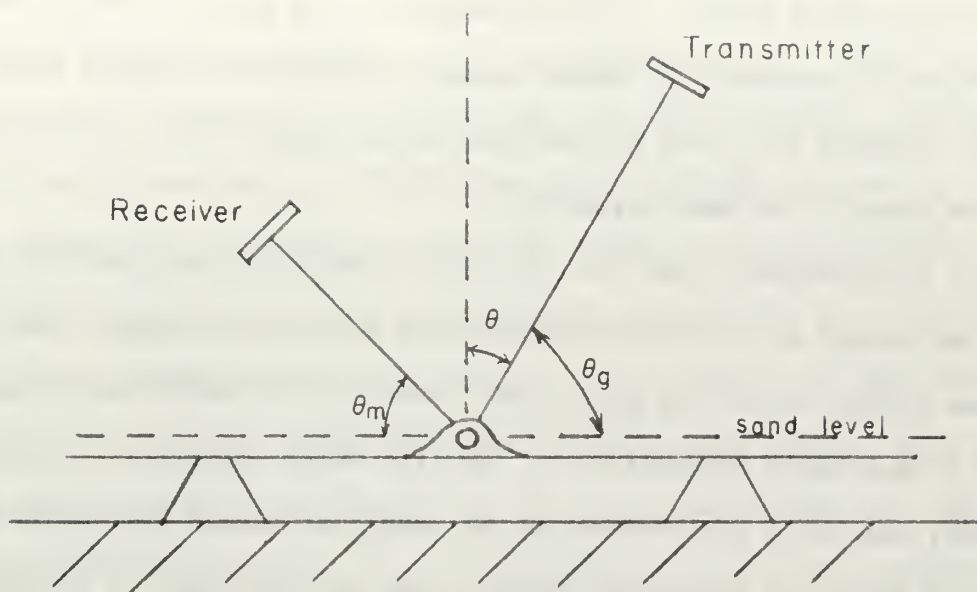material so that it could be easily driven through its 180 degree radial

16

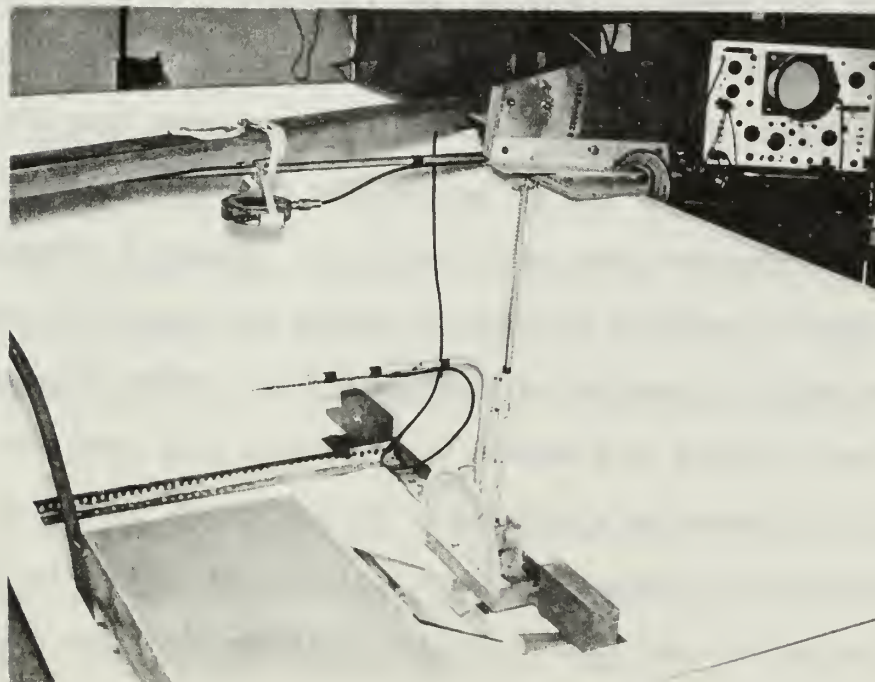Figure 3.1 Diagram of Transducer Supports

Figure 3.2 Experimental Apparatus

traverse by an electric motor. The motor and traverse arm were connect-
ed by gears and a chain. A potentiometer on the gear box shaft was
calibrated to provide a DC output proportional to the angular position
of the traverse arm. Due to backlash in the chain drive, all the travers-
es were made in the same direction.

An aluminum box, four feet by one and one-half feet and five inches
deep was placed at the bottom of the tank within the support frame. The
box was filled to the top with fine (30 mesh) "Del Monte White Sand" pro-
duced by Del Monte Properties Co., Pacific Grove, California. The top of
the box, and hence the surface of the sand, was placed level with the
shaft on which the transducer support arms were rotated. A photograph of
the experimental apparatus is shown in Figure 3.2.

Transducers

The requirements placed on the transducers for this experiment were
extreme. First, a wide band device was required because of the desire
to investigate the problem over the frequency range from 100 kcps to
350 kcps. This range was set by the size of the most easily made ripples
and by the electronic equipment available. Second, a reasonably narrow
beamwidth was required in order to confine the insonified reflecting sur-
face to within a sand box of reasonable size. Twenty degrees (null to
null) was selected as a maximum beam width as this insonified an area
25 cm. in diameter at a distance of 72 cm. Third, it was necessary to
insure that the transducer was not so large that the reflecting surface
would be in the near field. Kinsler indicates that near field effects
do not extend beyond a range

$$r \approx 2a^2/\lambda$$

a = transducer radius

λ = acoustic wavelength

for a free piston transducer. [8] In order to allow a safety margin, the transducer radius was selected such that $2a^2/\lambda$ never exceeded 50 cm.

Attempts were made to obtain commercial transducers having the desired beamwidth and frequency response. None were available and a series of locally constructed mylar electrostatic transducers was employed. This type of transducer is very inexpensive to build, has wide bandwidth and essentially free piston-like directivity capabilities. [16] In order to meet both the beamwidth and far field conditions in a water depth less than three feet, it was necessary to employ two different transmitters. One had a radius of five cm. and the other 3.5 cm. The larger transducer was used at frequencies from 100 kc to 150 kc, and the smaller one from 200 kc to 350 kc.

In order to insure that spherical divergence was occuring, sound pressure level measurements made along the transducer axis were plotted against frequency on semi-log paper. When this curve approached within one db of its final six db per octave slope, far field performance was assumed. These measurements indicated that the far field began at a range ten percent greater than the $2a^2/\lambda$ indicated above. Examples of the directivity patterns of the transducers are shown in Figures 3.3 and 3.4.

It was not initially intended to be concerned with the absolute magnitudes of the spectra amplitudes; the main concern being with the relative amplitudes of the various spectra. However, in order to draw conclusions as to the effect of frequency on the scattering phenomenon
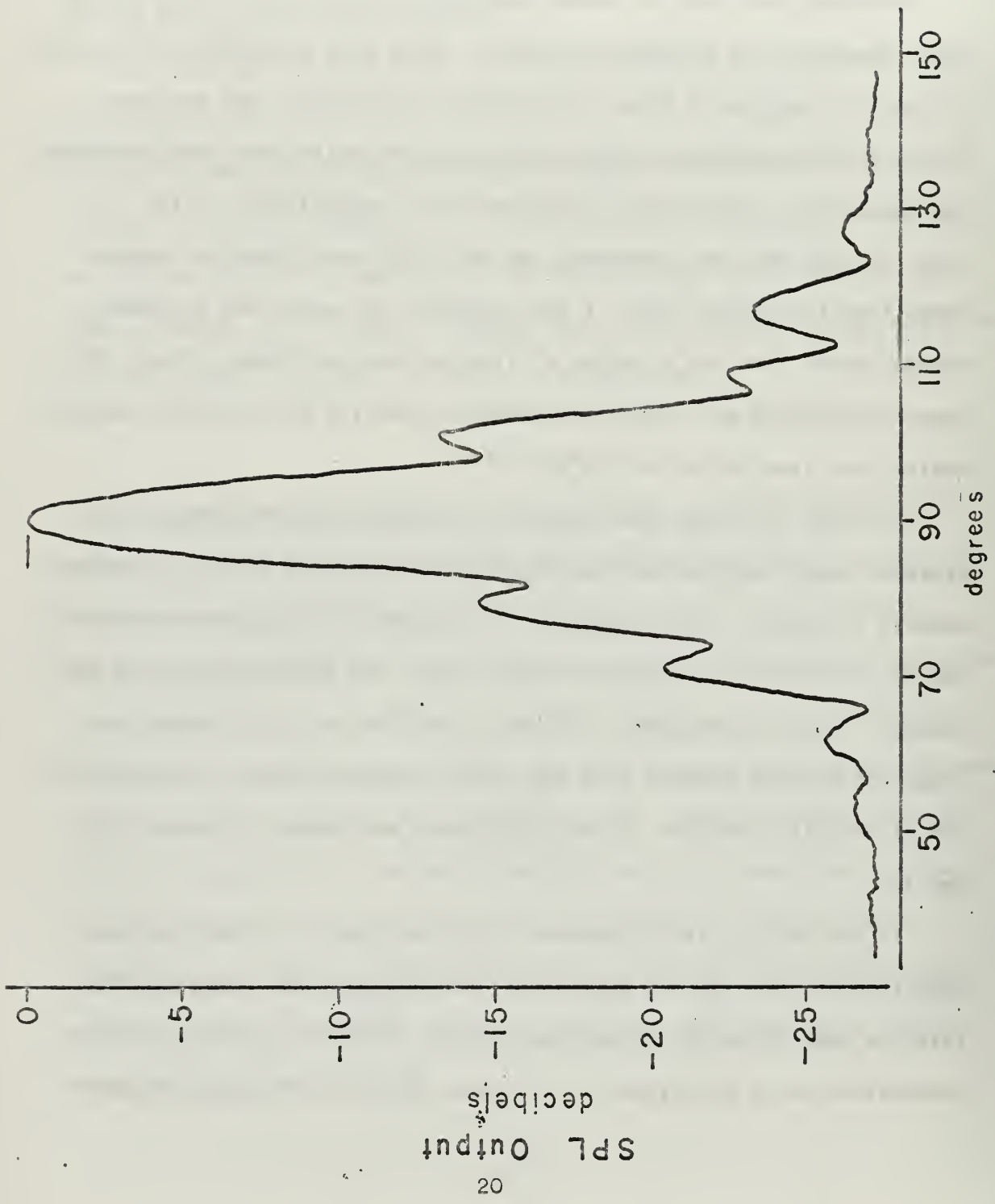
19

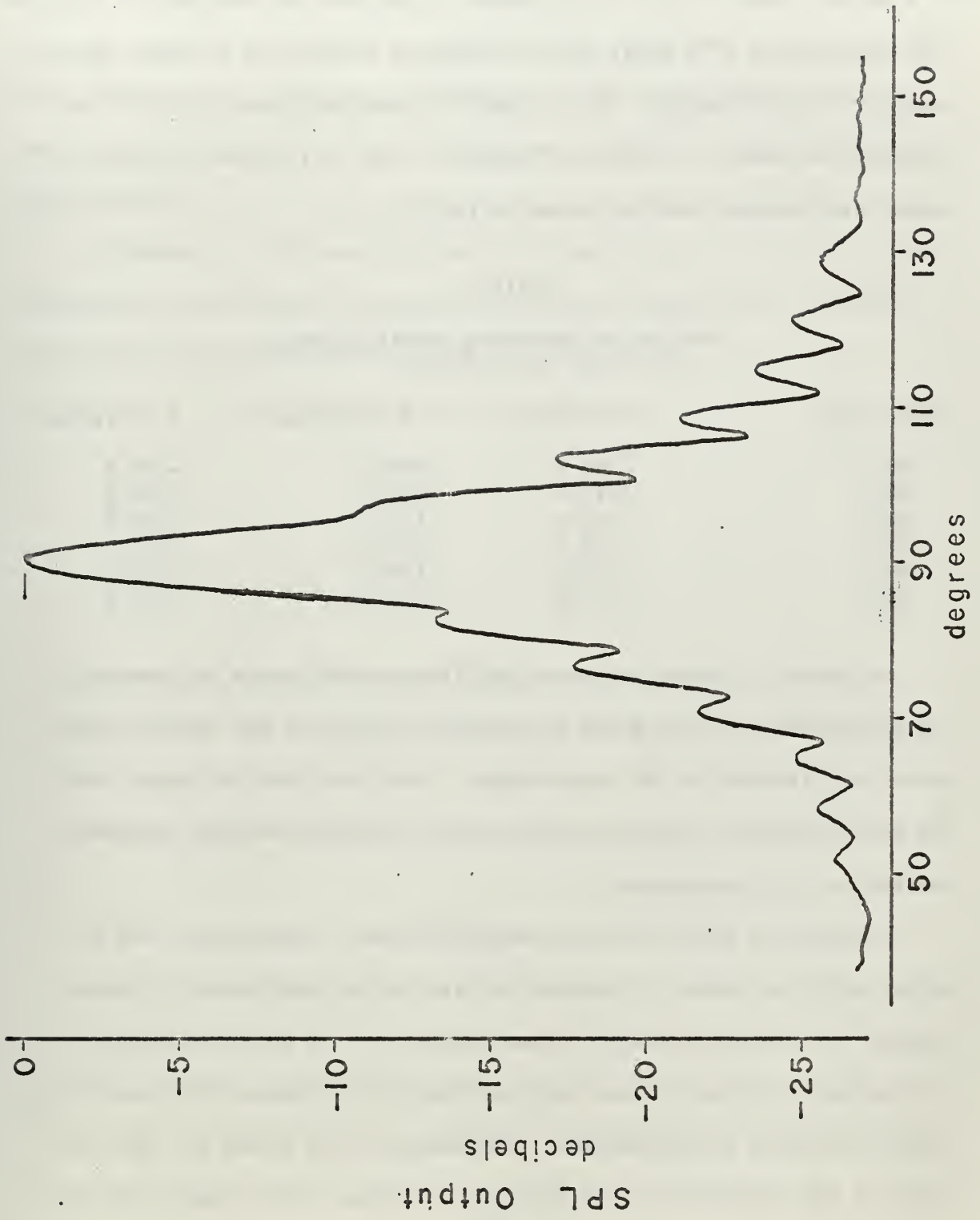Figure 3.3 Directivity Pattern of 5 cm. radius Transducer at 100 kc.

Figure 3.4 Directivity Pattern of 3.5 cm. radius Transducer at 200 kc.

it was deemed necessary to determine accurately the relative sensitivity of the receiving transducers. This was accomplished by substituting the hydrophone to be calibrated in place of a previously calibrated standard in a pulsed sound field. The standard hydrophone was obtained by reciprocity calibration of a small mylar transducer being used on other experiments by G. L. Palatini. [16] Since the absolute sensitivity of the standard was known, the absolute sensitivities of the receivers and the probe were obtained and are shown in Table I.

Table I

Transducer Receiving Sensitivities
(db re   1 /ubar)

freq. (kc)	1/8" probe	3.5 cm radius	5 cm radius
100	-130.0	-106.5	-106.6
150	-127.6	-110.9	-109.6
200	-125.0	-117.4	-112.4
250	-128.8	-118.8	-114.4
300	-135.0	-119.9	-115.6
350	-137.8	-121.1	-115.2

In order to obtain reflected amplitudes which could be compared, the calibrated 1/8 inch probe was placed in front of the source transducer at a distance of 60 centi-meters. This was used to ensure that the Sound Pressure Level incident on the reflecting surface remained constant at all frequencies.

Attempts to calibrate the transmitters were unsuccessful due to being unable to ensure a constant DC bias on the electrostatic transducers. The mylar gradually became polarized in a direction opposite to the applied field and it was very difficult to determine the exact "effective" bias on the transducer. Fortunately this effect was much reduced on the transducers used only for receiving. The reasons for this

are not clearly understood. Measuring the sound field directly as mention-
ed above obviated any requirement for calibrated transmitters.

It is interesting to note that the small probe made from a 1/8 inch
barium titanate cylinder was far from omnidirectional even at frequencies
as low as 100 kc. In addition, the directional pattern varied radically
with frequency. A specific orientation of the probe was selected and
once it was calibrated, this position was carefully preserved during all
measurements.

Alignment of the apparatus and the transducers was found to be most
important in assuring an accurately calibrated experiment. Incorrect
tilt of one transducer gave as much as 2 db. error.

Transmitter

A transmitter block diagram is shown in Figure 3.5.

The acoustic pulses are generated by feeding the output of a Hewlett Packard test oscillator Model 650A into a General Radio Tone Burst Generator Model 1396A. The Tone Burst Generator is essentially a transmitter gate which can be set to open for a selected number of cycles and remain closed for a selected period composed of an integral number of cycles. The gate is coherent in that the tone burst always begins and ends at the same point in a cycle of the input signal. A pulse length of 16-64 cycles (depending on frequency) was selected as being long enough to set up reasonably steady-state conditions during the pulse. A low pulse repetition frequency of 40 Hz was used to avoid interference among the pulses in the highly reverberant steel tank.

The Tone Burst Generator provided only 44 db. isolation between gate-open and gate-closed conditions. This permitted a substantial standing wave background noise which restricted the dynamic range of the experiment. Satisfactory isolation was obtained by feeding the Tone Burst output into a second gate, the schematic for which appears in Figure 3.6. This gate is essentially a shunt-chopper and is a somewhat less refined version of the General Radio Tone Burst Generator. The gate trigger is obtained from the "gate out" terminal of the tone burst generator which provides a large positive voltage except when the gate is open. The negative on-signal turns off the shunt transistor and the input is fed directly to the output. When the transistor is "on" its impedance is under 40 ohms and the signal is essentially shorted to ground. The input emitter-follower and the collector resistors provide a means of completely eliminating any pedestal effects by providing

24

Figure 3.5
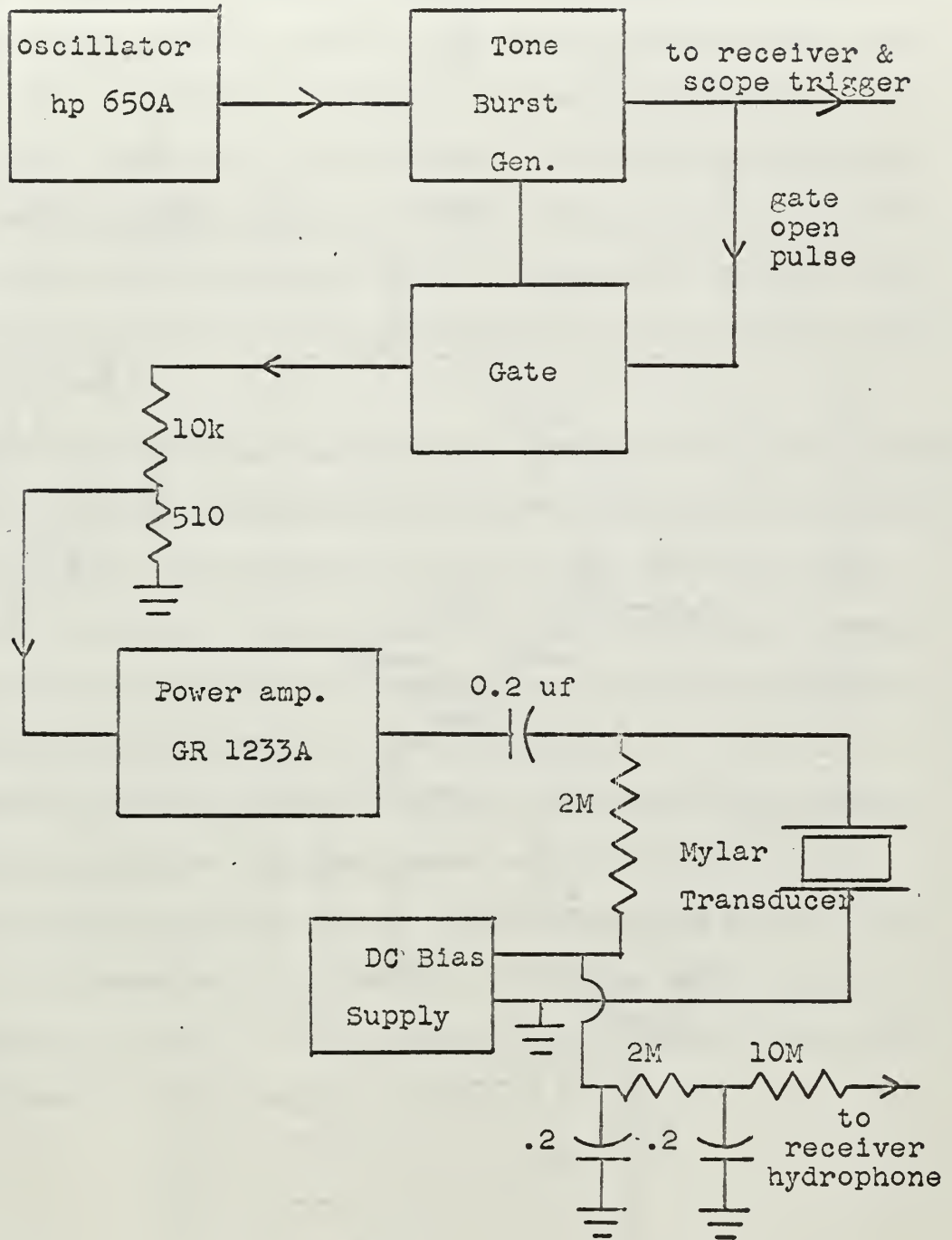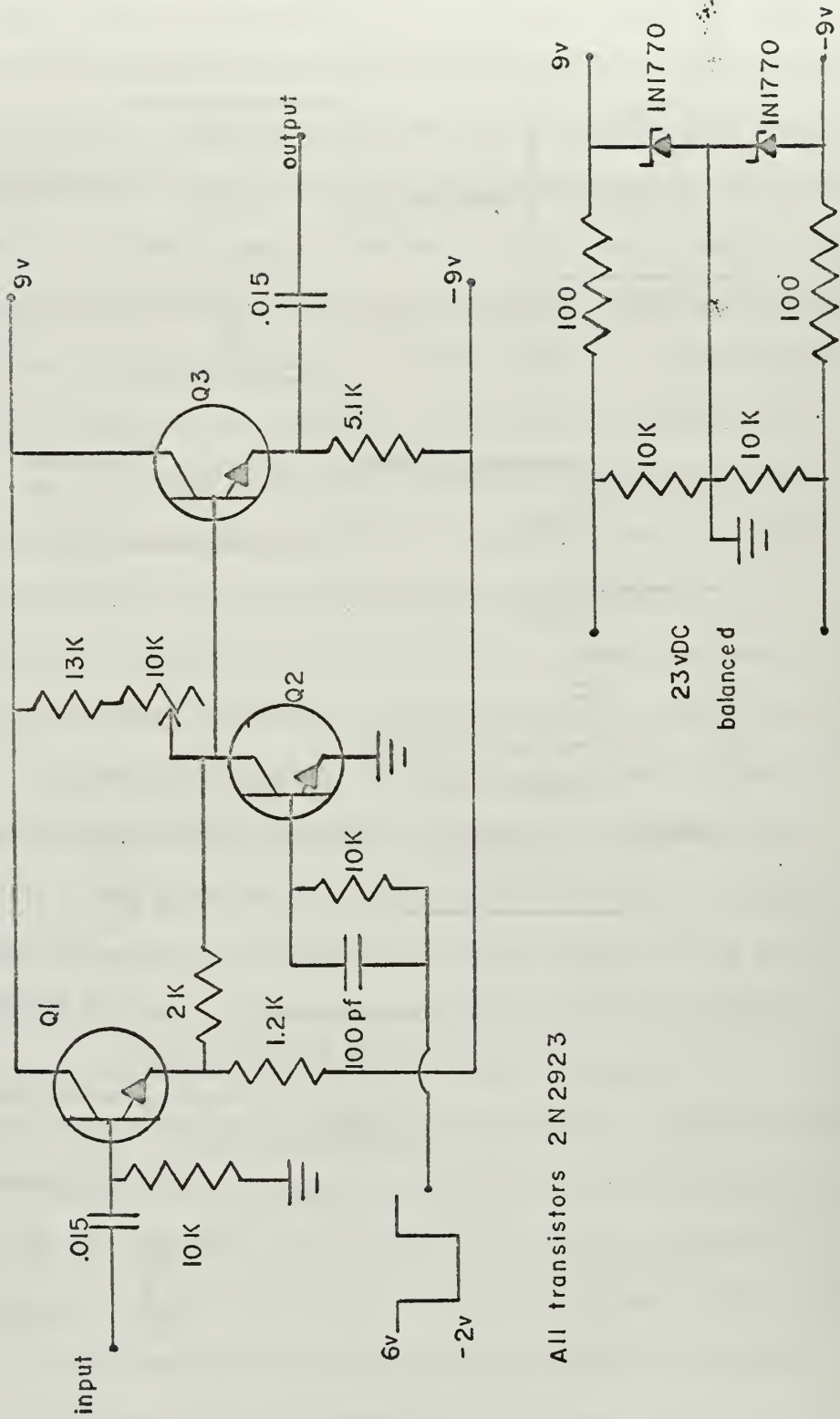
TRANSMITTER GATE

Figure 3.6

equal current through the collector resistance during both transistor on and off periods. The second emitter-follower provides isolation from external loading effects.

The reference diodes provide additional regulation on the power supply. The small "speed-up" capacitor in parallel with the current limiting 10 kilohm resistor reduces delay in the opening and closing of the gate. Slight improvement in operation might be obtained by elimination of the input and output capacitors if the circuit is not to be used with tube circuits where high voltages might be encountered. Through use of the two gating circuits in series, an isolation of over 75 db was obtained.

Significant switching transients were present in both gating circuits and it was necessary to operate the oscillator at reasonably high levels. Only a high gain power amplifier, the General Radio Model 1233A, was available, so a 20 to 1 voltage divider was inserted between the gating circuits and the power amplifier input in order to obtain a compromise between the desired output and minimum transients.

Variable DC Bias, between 160 and 300 volts, for the mylar transducer was obtained from a Hewlett-Packard model 710 power supply. A blocking capacitor served to isolate the power amplifier and the power supply. A 2 megohm resistor in series with the bias supply provided current limiting in event of a short and eliminated shorting of the output signal through the power supply.

27

Receiver

The receiver block diagram is shown in Figure 3.7. The output of the receiving transducer was fed to a battery powered transistor amplifier, Burr-Brown Model 100. This unit, set for 20 db gain, was selected as the first amplifier because of its low noise characteristic, thus assisting the establishment of a high signal to noise ratio early in the receiver chain.

The second amplifier utilized was a Hewlett Packard Model 465A transistor preamplifier set at a gain of 40 db. This amplifier was also selected for its low noise capability.

At this point variable filtering was accomplished by placing in series the two sections of a Spencer-Kennedy Labs Model 308 dual electronic filter. This permitted both high and low pass filtering at an 18 db per octave rate. In the higher frequency experiments, the low pass filtering was omitted.

The filtered signal was observed and the experiment monitored on a dual-beam Tektronics 565 oscilliscope. Care was taken to ensure that the filters did not remove information useful to the experiment.

The output of the filter was further amplified by 20 db in a Scott Model 140A amplifier and fed to a receiver range gate. This gate was constructed similarly to the transmitter gate. The schematic is shown in Figure 3.8. The two shunt-choppers yield an isolation between gate-open and gate-closed in excess of 60 db. The gating signal amplifier, Q6 serves to match the gating signal input to the output of the Digital Equipment Corporation Laboratory Modules which provide the delays and pulse forming circuitry required for the input pulse. The delayed input
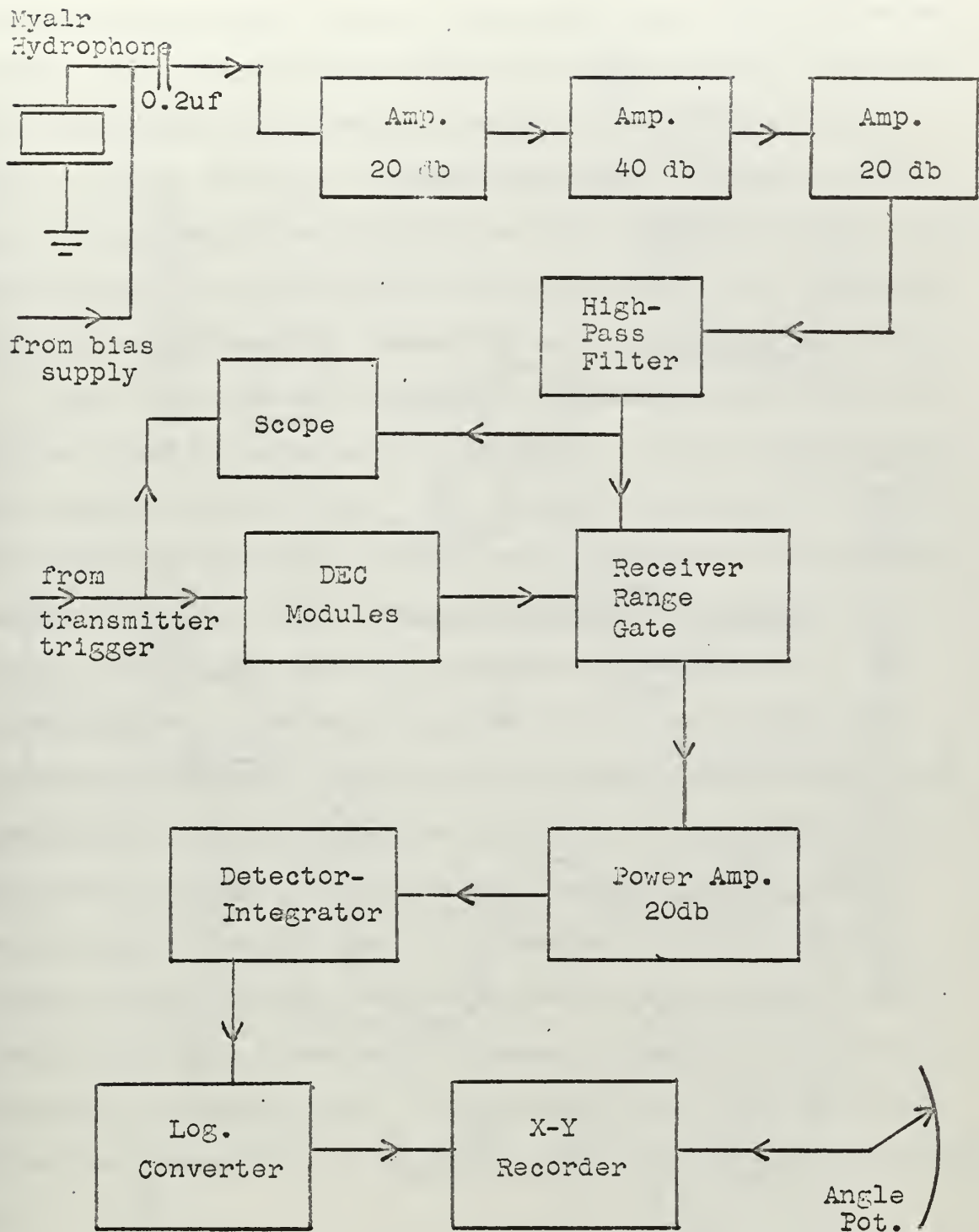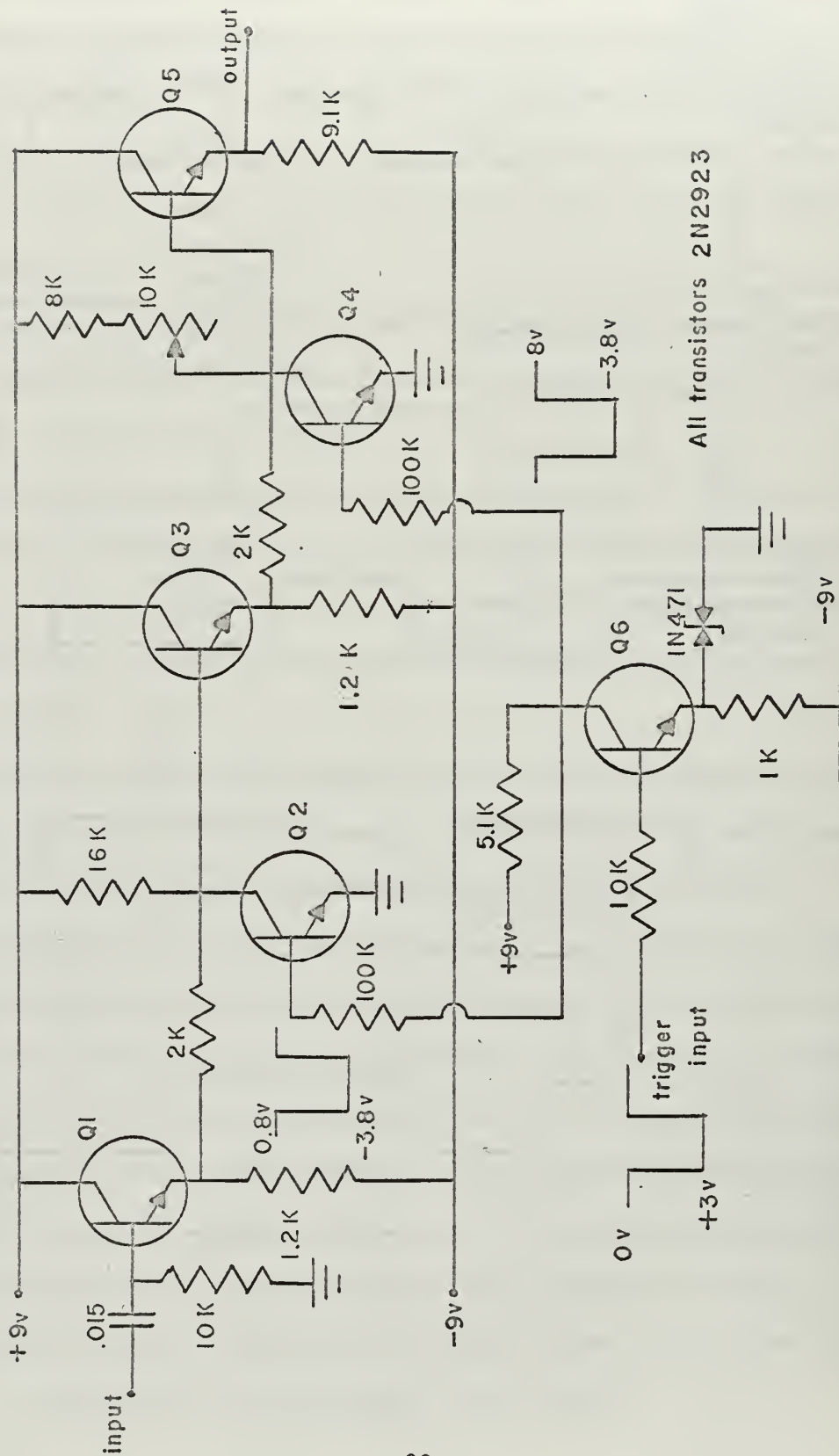
28

Figure 3.7 Receiver Block Diagram

RECEIVER RANGE GATE

Figure 3.8

All transistors 2N2923

30

pulse is formed in the DEC modules by differentiating the Tone Burst Generator gating signal forming a very narrow pulse. This pulse passes through a variable delay circuit and changes the state of a "flip-flop." The delayed pulse also passes into another variable delay circuit and then is used to return the flip-flop to its original state at a later time. By appropriate setting of the two delay circuits the output of the flip-flop serves to position the receiver range gate over a considerable range (up to approximately 1 second) in both time delay and gate width.

Use of the range gate provided very accurate selection of the reflected signal to the exclusion of any noise or spurious response which are separated from it in time. Thus automatic processing and recording of only the reflected pulse is facilitated. The output of the gate was amplified 20 db by a Hewlett-Packard Model 467A power amplifier which drives a simple diode detector and integrator. See Figure 3.9. The combination of very low duty cycle (under 0.5%), long charging time constant (approximately .0012 sec) and very long discharge time constant provides a DC output with very low ripple and a linear characteristic over more than 40 db. In addition the integration circuit provides nearly complete immunity from all random noise and all but very low frequency periodic noise. Spurious response is also avoided by operation of the receiver range gate at a signal level where the switching transients are insignificant. Bias for the detector diode is provided by setting the gate so that the output "rides" on a small positive pedestal.

The DC voltage from the integrator was read on an RCA Senior Voltohmyst and on the vertical scale of a Moseley X-Y recorder. Since the

31

DETECTOR-INTEGRATOR
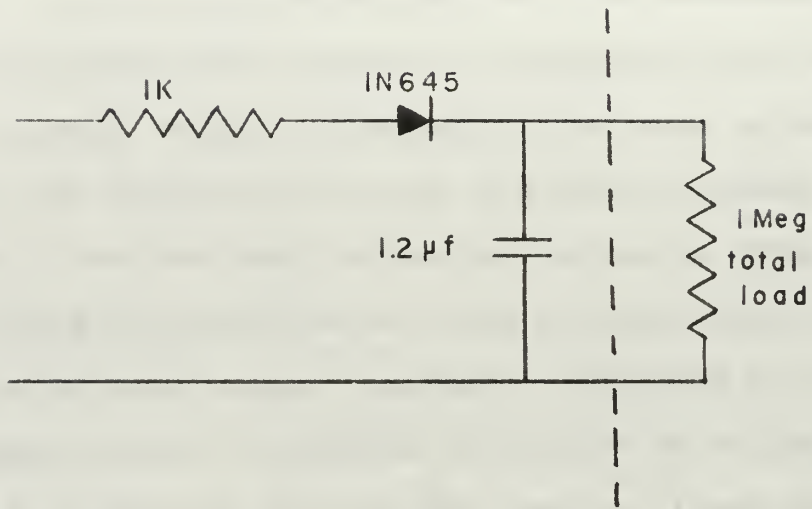
Figure 3.9
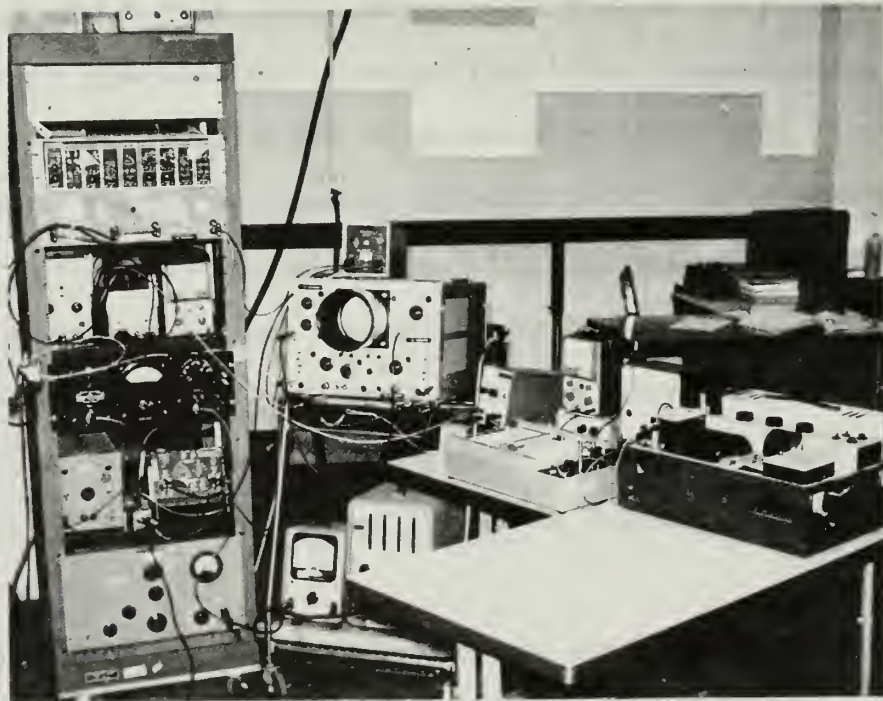
Figure 3.10 Electronics Equipment

X-Y plotter has a linear scale, a Moseley Logarithmic Converter Model 7561A was used to provide a decibel reading. The horizontal scale of the X-Y plotter was calibrated in degrees with deflection provided by a precision potentiometer connected to the shaft of the traverse-drive motor. Power for the potentiometer was provided from the same regulated DC power supply as the gates.

A photograph of the electronic equipment as used in the laboratory is shown in Figure 3.10.

4. Preliminary Observations

In order to check out the equipment, tests were made at normal incidence using a large piece of styrofoam as the reflecting surface. The styrofoam was weighted so that it could be placed at the bottom of the tank in place of the sand. A clear undistorted reflected pulse was obtained and a radial traverse indicated that the reflected pulses accurately mirrored the directivity pattern of the transducer. However, a reflection coefficient significantly greater than one was obtained. The method was tested by turning the experiment over and using the water-air interface as a reflecting surface. This procedure yielded a reflection coefficient very close to one as expected.

Experiments with flat sand also yielded a clean undistorted reflected pulse. An oscilloscope trace of this pulse is shown in Figure 4.1. An angular plot, Figure 4.2, indicated that the reflected pulses accurately mirrored the directivity pattern, but here again the reflection coefficients were unusually high, ranging between 0.8 and 1.5. Predicted reflection coefficient for the flat sand is 0.40, using the measured density of 2.01 gm/cm^3 and Nolle's speed of 1.74×10^3 meters/sec. [14] This velocity was later confirmed as reasonably accurate for this experiment when the critical angle was experimentally determined to be approximately 57 degrees plus or minus one degree.

Poking the sand with a pole revealed a large number of small air bubbles trapped in the sand. Removal of some of these bubbles by stirring the sand destroyed the clean shape of the reflected pulse. As can be seen in Figure 4.3, several distinct reflections appear from within the sand volume. Before stirring, the dense, relatively uniform concentration of bubbles presented a flat upper surface which effectively
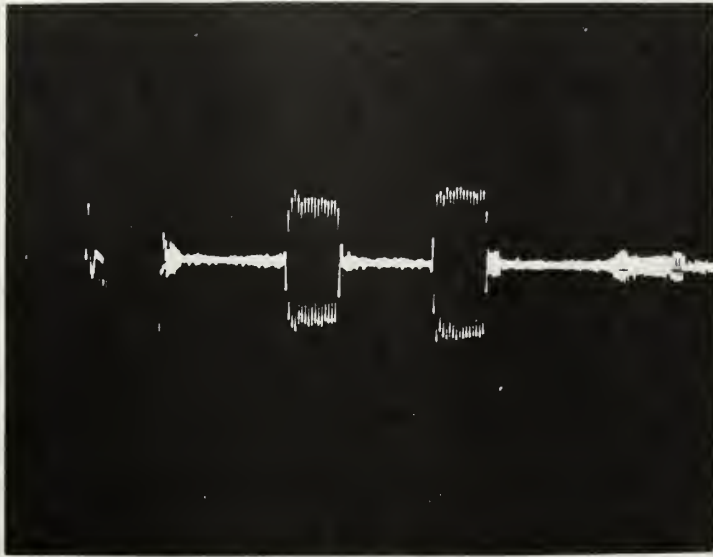
34

Figure 4.1 Flat Sand Reflection (before boiling)

      1) Sand Surface Reflection

      2) Sand Surface--Water Surface Reflections

      3) Sand--Air--Sand Reflections

        16 cycles at 100 kc.

        vertical scale 0.2v/cm.
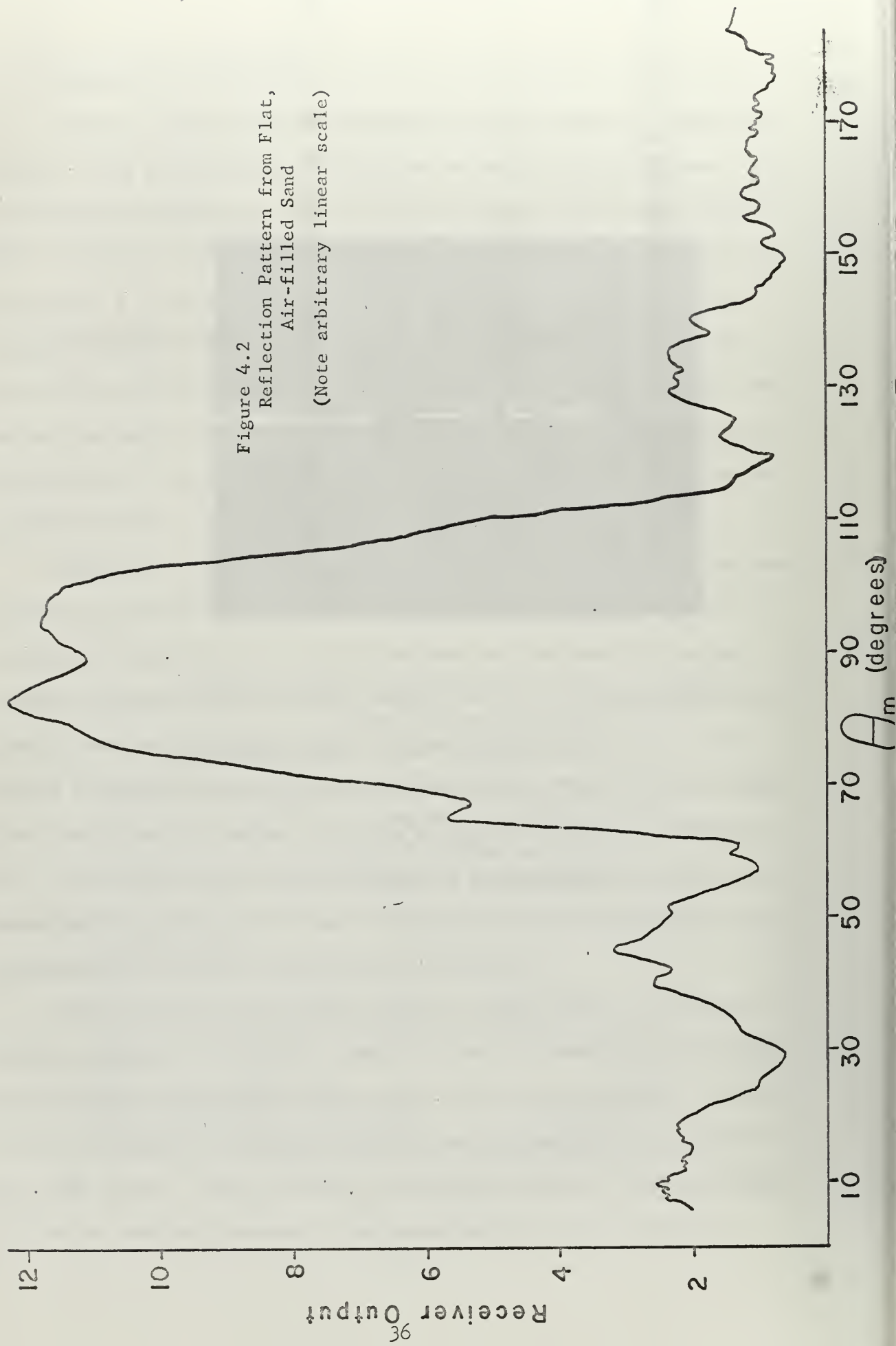
        horiz. scale 0.2 ms/cm.

Figure 4.2
Reflection Pattern from Flat,
Air-filled Sand

(Note arbitrary linear scale)

reflected nearly all the incident energy and allowed almost none to penetrate into the volume of the sand. This led to the clean undistorted pulse of Figure 4.1. After stirring, the bubbles were less dense, and the sound entering the sand was reflected both from the irregular upper surface of the bubbles and from areas where the bubbles were more highly concentrated. This volume scattering from within the sand made it impossible to obtain a usable undistorted pulse which was reflected only from the sand surface.

Angular traverses made using the sand in this condition gave wildly random reflection patterns bearing little resemblance to the appropriate reflected directivity pattern of the source. An example of such a traverse is shown in Figure 4.4. Similar plots were obtained regardless of the condition of the sand surface; flat, rippled or randomly scored. It is apparent that neither Figure 4.2 nor 4.4 is a true plot of the reflections from the sand surface, but from the sand volume or from the surface of the layer of bubbles.

The most significant indication of volume scattering is the fact that a distinct reflection was not received from the bottom of the sand. Apparently the sound was being completely reflected prior to reaching the sand bottom.

Barnard discusses elaborate precautions taken with his sand mixtures, and Nolle mentions large reflection coefficients which occur when the sand is not boiled, but neither discusses the severe interference discovered here. [1,14] Following their lead the entire 600 pounds of wet sand was boiled over a gas burner in a large drum (200 pounds at a time) and transferred to the bottom of the water tank. The boiled sand was

37

Figure 4.3 Reflected Pulse from Flat, Stirred Sand

1 cycle at 100kc. Normal Incidence

The top trace shows electronic pickup from the transmitter, direct unreflected pulse, sand surface reflection, and sand surface--water surface reflections.

vertical scale 0.5v/cm. horiz. scale 0.2ms/cm.

Several pulses of volume scattering can be observed on the bottom trace between the sand surface reflection and the small indistinct reflection indicating the sand box bottom approximately 3 cm. after the large surface reflection.

vertical scale 0.05v/cm.
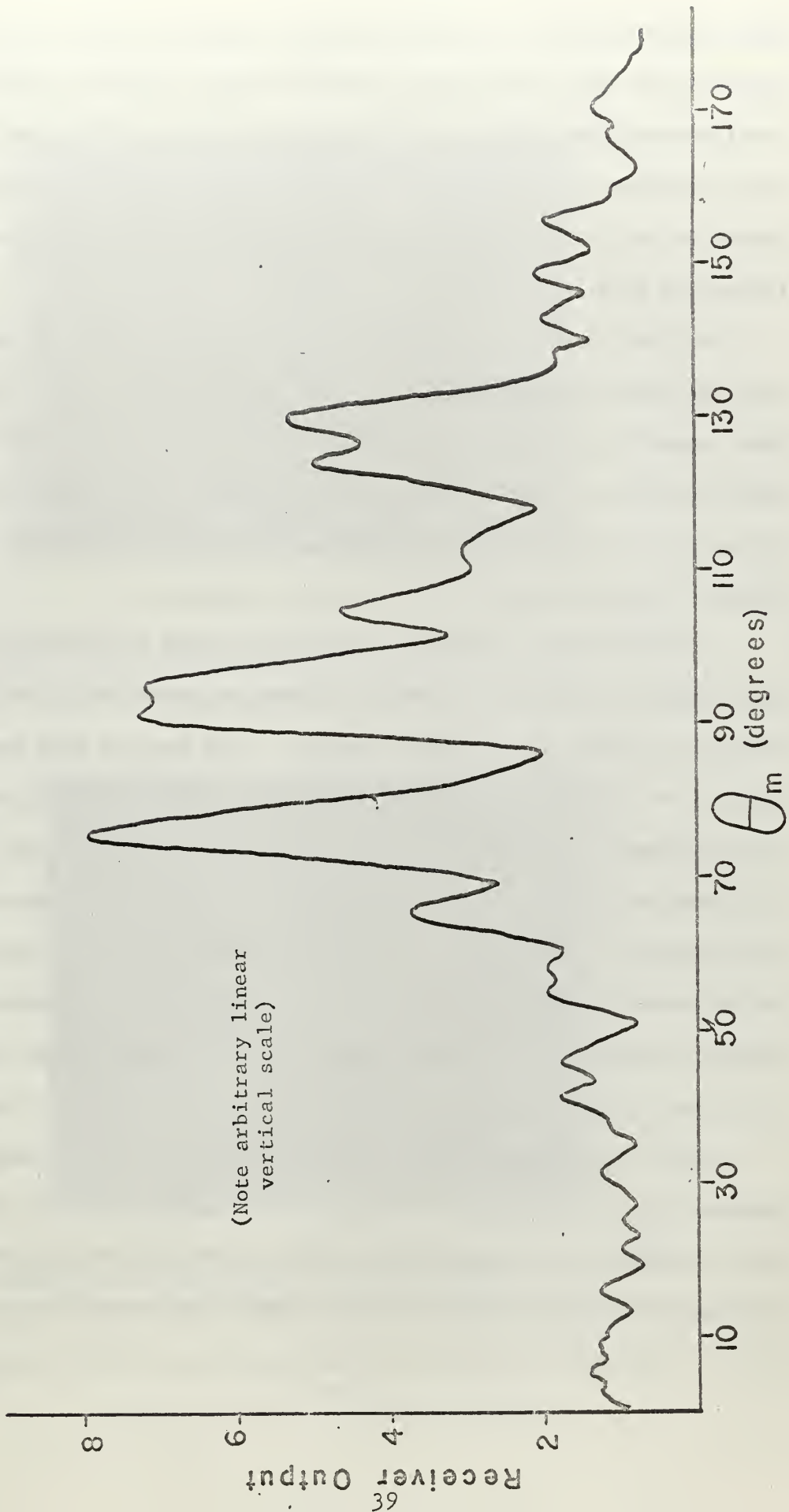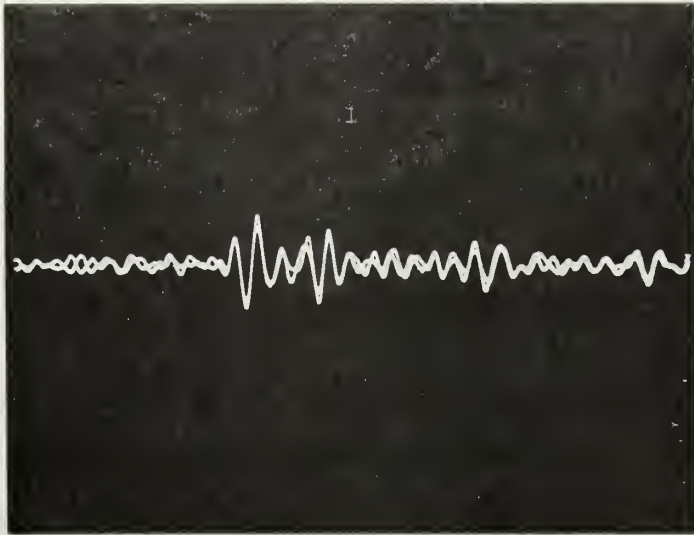
horiz. scale (approx) 30 usec/cm.

Figure 4.4 Reflection Pattern from Flat, Stirred Sand $\theta_g = 90°$

(Note arbitrary linear vertical scale)

Receiver Output

θ_m (degrees)

kept under water at all times during the transfer process. Boiling re-
moved all the air from the sand and the volume scattering disappeared.
Oscilloscope photographs of early test samples of unboiled and boiled
sand are shown in Figure 4.5. Note the repeated echoes and indistinct
bottom return in the unboiled sand, and the distinct bottom return in
the boiled sand.

As might be expected this procedure rendered reflection coefficients
near the predicted values. It is felt that the air bubbles in the sand
were resonating at the acoustic frequencies used, thus acting as scat-
terers having an effective cross-section hundreds of times larger than
the actual cross-section. In addition it is hypothesized that the
bubbles in the submerged styrofoam acted similarly.

It was initially intended to utilize a small omnidirectional receiv-
ing probe, since this is a simple lightweight device which could easily
be driven through the intended traverse. This was the type receiver
used by Yen and Middleton. [22] During use of the 1/8 inch probe des-
cribed in section three, it was determined that the probe was receiving
reflected energy from many directions. This could be observed on the
oscilloscope as a considerable amount of distortion of the received
pulse caused by phase interference as a result of the different path
lengths traveled by the undesired pulses. The desired pulse could not
be cleaned up sufficiently even through use of the receiver range gate.

When a directional receiver was used, much cleaner pulses were
received virtually without distortion. The amplitude plots as a func-
tion of angle were far more noise-free, and the fine structure caused
by phase interference distortion was almost eliminated. This occurred

a) Unboiled sand has small surface reflection, considerable
   volume scattering and indistinct bottom reflection.

   vertical scale 0.05v/cm.   horiz. scale (approx.)25us/cm.
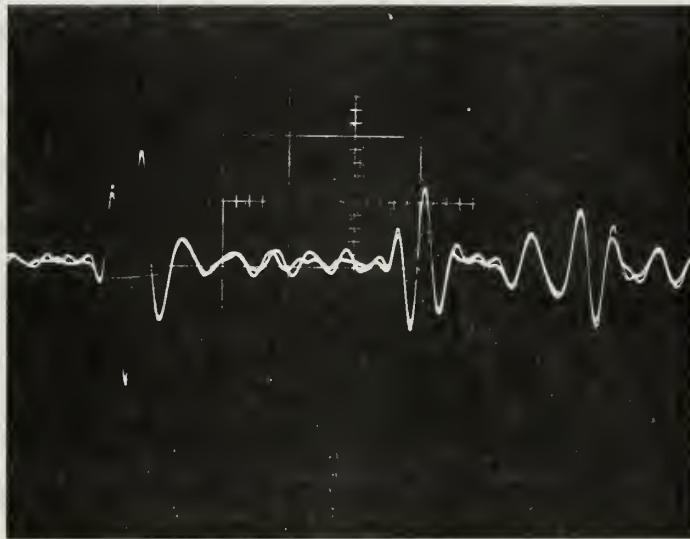
b) Boiled Sand has larger surface reflection and a clearly
   defined bottom reflection 4 1/2 cm. later.
        vertical scale 0.05v/cm.   horiz. scale 0.02ms/cm.

Figure 4.5 Reflected Pulses from Flat Boiled and Unboiled
                        Sand
           1 cycle at 100kc.   Normal Incidence

even when a receiver having a beamwidth twice that of the transmitter was employed. Little change was noticed when a narrower beam receiver was used. However, identical transducers were used for receiver and transmitter whenever possible.

It is believed that the omnidirectional probe-type receiver can be used only if its range from the reflecting surface is very much larger than the dimensions of the insonified surface. The experiments of Yen and Middleton do not seem to have met this criterion. An exception to this condition would certainly occur if one desires to study the sound field close to the surface. (Papadakis discusses measurements in air within the near field of a periodic surface). [17] It was the aim of this model experiment to draw mainly what one might call "far-field" conclusions.

After the equipment was checked out thoroughly and operating proper-ly, radial traverses were made through the sound field reflected from flat sand. Angles and frequencies utilized were the same as those to be used for the experiments in rippled sand: 90°, 70°, 45°, 30°..100, 150, 200, 250, 300, 350 kilocycles. These flat sand runs were made at a constant power output from the transmitter as described above, and permitted a useful comparison of the spectral (zero order) reflection between rippled and flat surface. (See Figures 4.6 and 4.7).

Ripples, oriented perpendicular to the incident sound, were made on the sand mechanically by use of a cylinder having longitudinal cor-rugations. The cylinder was supported by plastic-tired wheels riding on the edges of the sand box. (See Figure 4.8). (The plastic tires helped eliminate skidding and hence irregular ripples). Ripple wavelengths of approximately 1.30 cm were obtained. Since the corrugations dipped down

42

into the sand about three-sixteenths of an inch, the locus of a point on the outer edge of a corrugation was a prolate cycloid. This caused ripples which had a predominantly sawtooth waveform. However, this deviation from a sinusoid appears to have changed the results little; the main effect being to cause the spectra on the less sloping side of the sawtooth to have a higher amplitude. This effect was confirmed when, upon reversing the ripples, the higher amplitude spectra reversed sides also. The majority of the data was taken with the ripples in the same direction for consistancy. Several runs were made at 45 degrees with the ripples in the opposite direction (i.e., sound hitting steep side of ripple crests).

In order to compare the experimental data with theory it was necessary to determine the parameters, λ_s and h, of the rippled sand surface. The wavelength, λ_s, was determined by measuring twenty ripples with a ruler and using the average. This yielded $\lambda_s = 1.23$ cm. The ripple height, h, was more difficult to determine. Attempts to use a depth gauge destroyed the ripples and may have led to errors in the measurement. These measurements resulted in h = .136 cm. Several materials were tried in an attempt to make a casting of the ripples and it was found that Portland Cement would harden under water if the top of the cement was exposed to air.

The casting was made with one inch of water covering the sand by sprinkling the dry cement-sand mixture (one to one) into a cylindrical form pushed into the sand surface. The semi-hardened cast was removed from the water after 12 hours, and when thoroughly dry, it was carefully brushed to remove excess sand.

43

Figure 4.6   Reflection Pattern from
Flat, Boiled Sand
$\theta_g=70°$
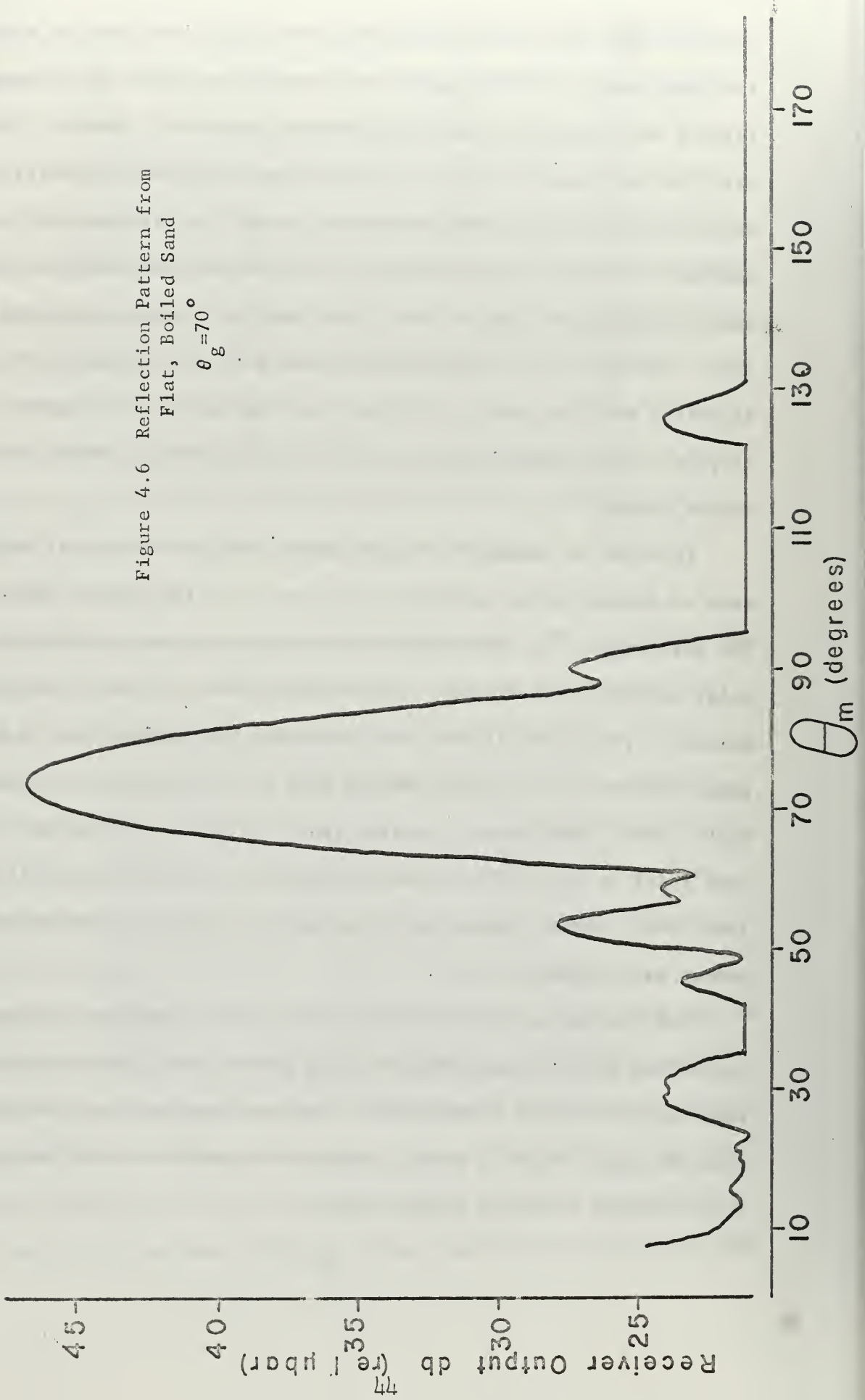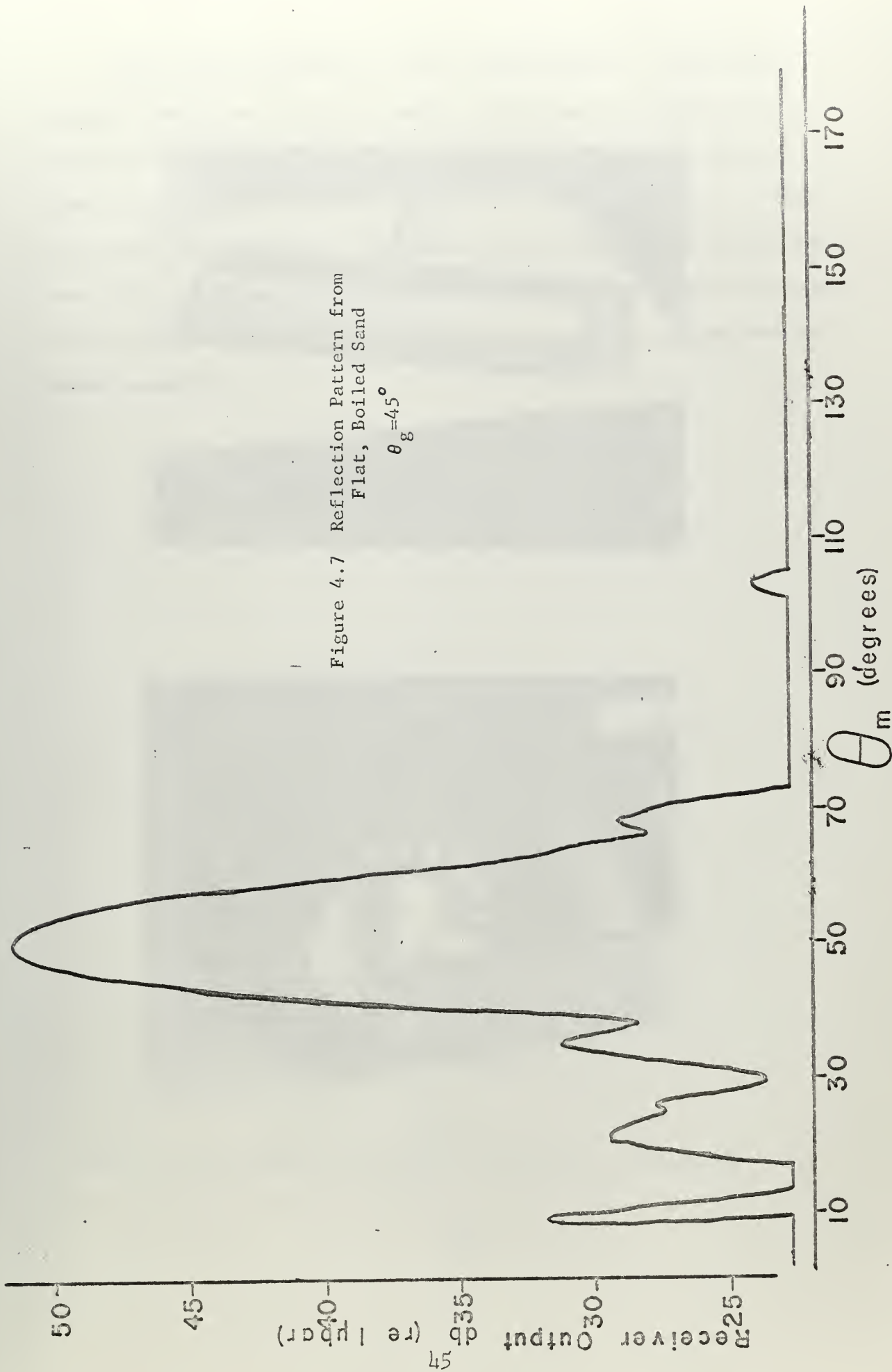
Figure 4.7   Reflection Pattern from
Flat, Boiled Sand
$\theta_g = 45°$

θ_m (degrees)

Receiver Output db (re 1 μbar)
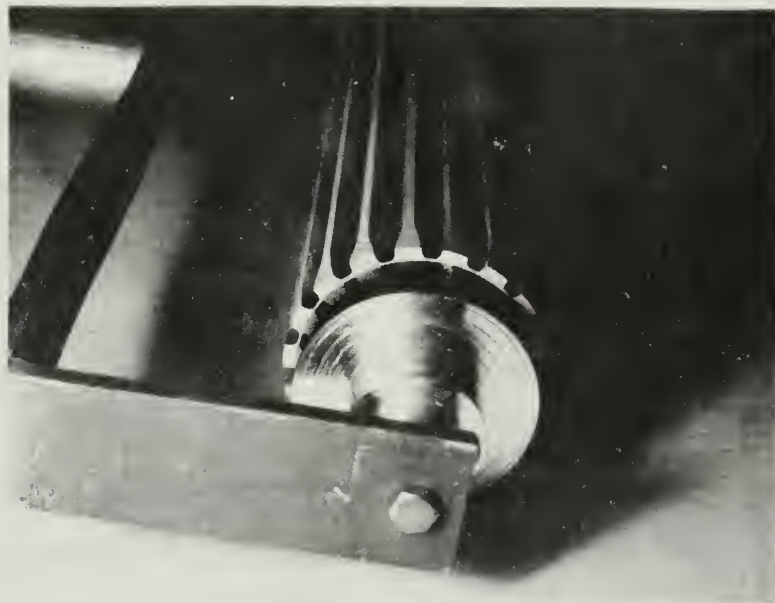
Figure 4.8 Corrugated cylinder for making sand ripples.

Depth gauge measurements on the casting gave h = .134 cm with a standard deviation equal to $\pm$ .006 cm. This result is only .002 cm different from that obtained from the depth gauge readings directly from the rippled sand surface. A sketch of the sand ripples is shown in Figure 4.9. As shown in the figure the crests occur at approximately one-third the distance between troughs. The sawtooth peaks were slightly more rounded than indicated by the sketch, and the ripples were assumed sinusoidal.
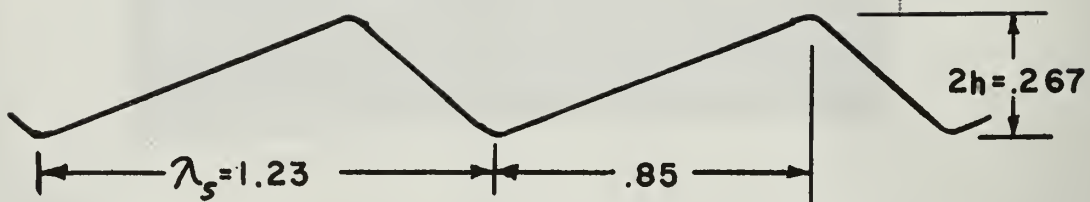
all dimensions in cm.

Figure 4.9   Sketch of sand ripples

5. Discussion of Results

Examples of radial traverses made by reflection from rippled sand are shown in Figures 5.1 through 5.4. The runs shown by these figures were all made at 300 kc at four different angles of incidence. The figures were copied directly from the recorder graphs without touch-up or removal of any bias.

The value $\lambda_s = 1.23$ cm was used to predict the direction of propagation of the scattered orders in accordance with:

$$a_m = a_0 + m\,\lambda/\lambda_s$$

as shown earlier. These predicted values are shown in Tables II and III along with angles obtained experimentally. A uniform bias determined from reflection experiments on flat sand has been removed from the experimental values in the table. This bias appears to be due to inaccuracies in the alignment of the apparatus.

Angles nearest cutoff for a certain order show the most deviation between theory and experiment due to the high degree of sensitivity of the cosine function at small angles. In fact, spectra which are predicted to lie just beyond cutoff at each frequency do in fact appear. This effect was apparently reasoned intuitively by Rayleigh when he mentioned, briefly, media which are not impenetrable. He gave no details of his reasoning.

The experimental spectra propagation angles are generally within two degrees of the predicted values. A few isolated cases of deviations as high as three degrees occur, but these are all at small angles.

From this data it is apparent that periodic ripples on a sand-water interface do indeed reflect energy according to theory; i.e.,

49

Figure 5.1 Reflection Pattern from Rippled Sand, $\theta_g = 90°$
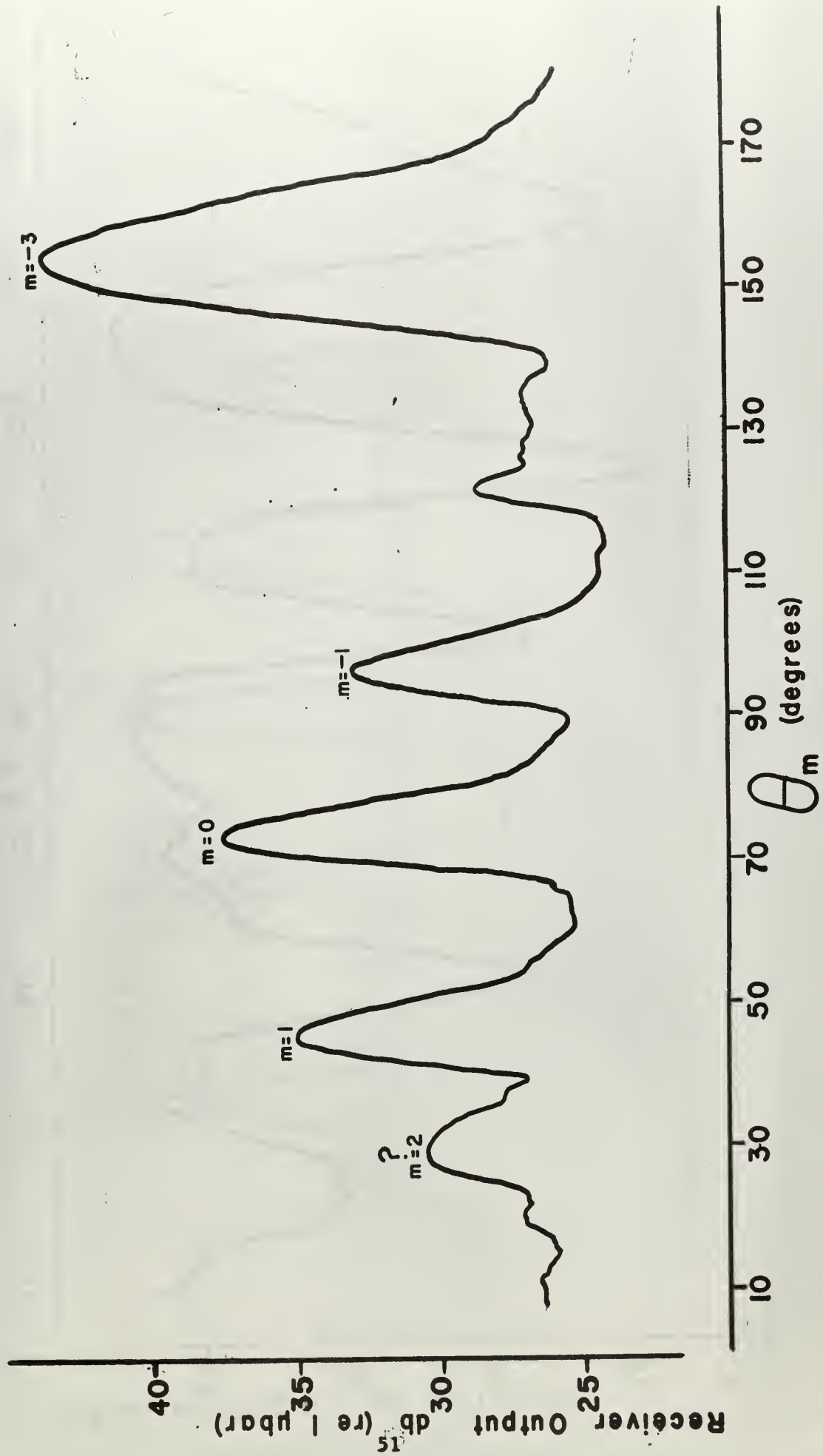
Figure 5.2 Reflection Pattern from Rippled Sand, $\theta_g = 70°$

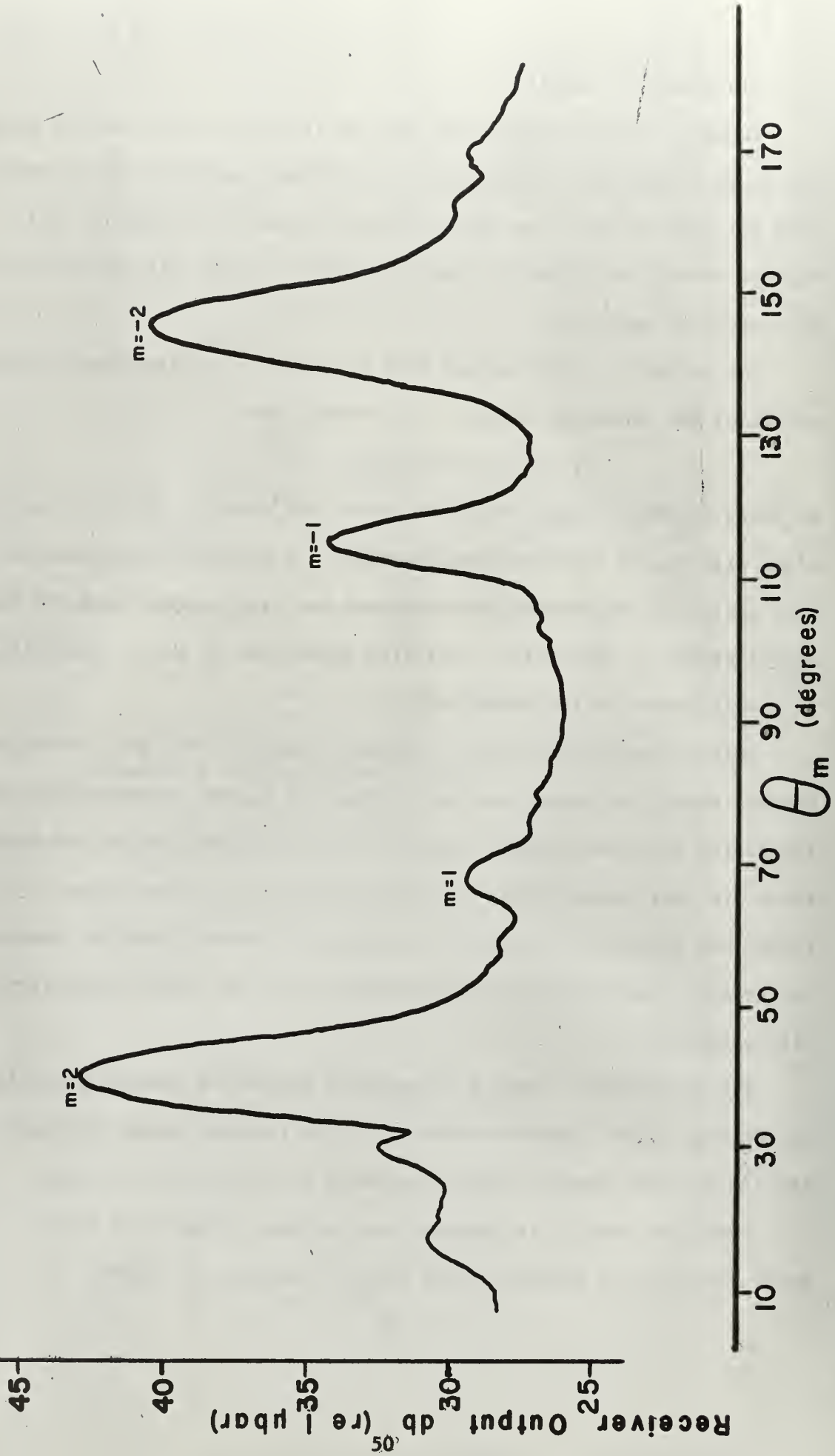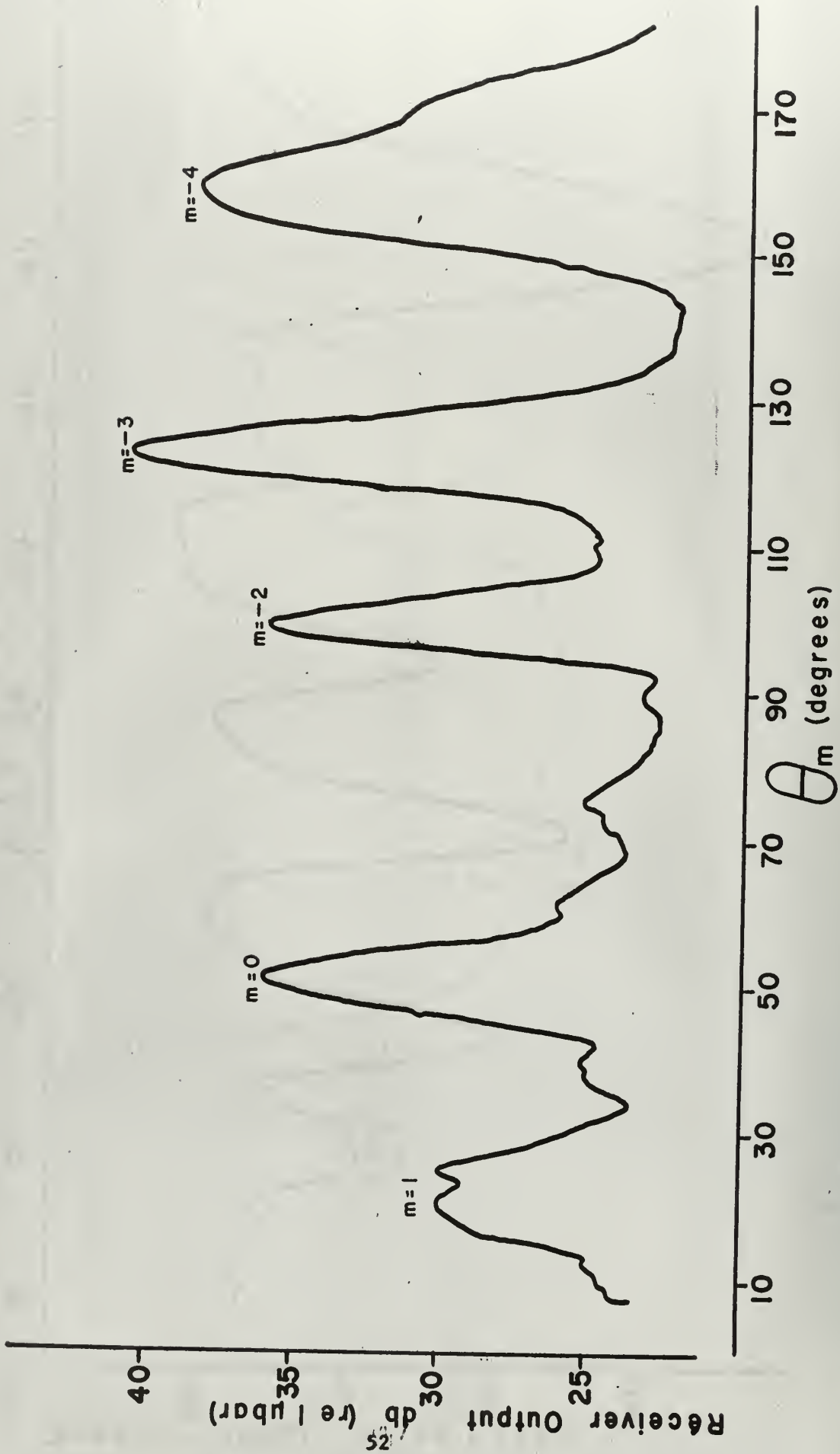Figure 5.3   Reflection Pattern from Rippled Sand, $\theta_g = 45°$
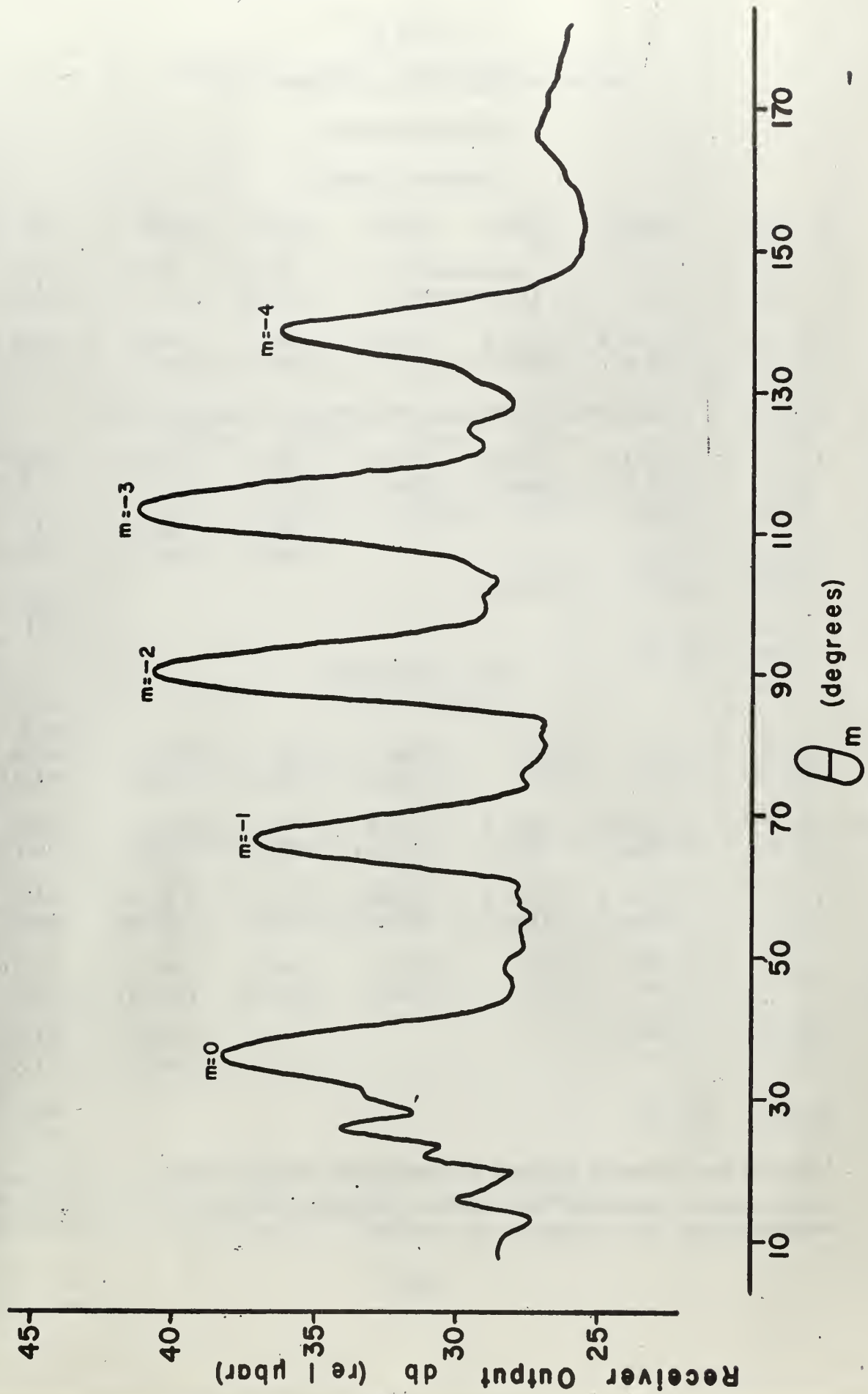
Figure 5.4   Reflection Pattern from Rippled Sand, $\theta_g = 30°$

Table II

Reflection Angle, Θ_m, (degrees) of mth

Normal Incidence

Frequency (kcps)

m	100	150	200	250	300	350
2		experimental (theoretical)		20.5 (17.0)	38.0 (37.1)	42.8 (46.8)
1	18.0 (*)	38.0 (37.2)	53.0 (53.2)	61.5 (61.4)	65.5 (66.5)	70.0 (70.0)
0	Spectral Reflection Obscured by Receiver Shadow					
-1	163.0 (*)	143.0 (142.8)	126.5 (126.8)	116.5 (118.6)	112.5 (113.5)	110.5 (110.0)
-2				162.0 (163.0)	143.0 (142.9)	130 (133.2)
-3						12 (*)

20° from Normal

m	100	150	200	250	300	350
2						15 (*)
1			20.0 (25.0)	35.0 (36.5)	42.1 (42.5)	46.8 (48.5)
0	69.0 (70.0)	69.5 (70.0)	70.0 (70.0)	70.0 (70.0)	70.0 (70.0)	70.0 (70.0)
-1	152.5 (148.5)	120.0 (117.2)	(**) (104.7)	95.0 (97.8)	93.0 (93.3)	89.5 (90.0)
-2			151.0 (148.5)	129.0 (127.9)	** (117.2)	** (110.0)
-3					151.5 (148.5)	133.5 (136.8)
-4						173.0 (*)

Spectra not shown at a given frequency are beyond cutoff

*Calculation indicates this spectra is beyond cutoff
**Transmitted pulse obscured by receiver

54

Table III

Reflection Angle, Θ_m, (degrees) of mth
Order Scattered Wave

45° From Normal

Frequency (kcps)

m	100	150	200	250	300	350
1					17 (*)	23 (*)
0	44.5 (45.0)	45.0 (45.0)	44.5 (45.0)	47.0 (45.0)	46.0 (45.0)	45.0 (45.0)
-1	116.0 (119.0)	93.5 (95.2)	81.5 (83.8)	75.5 (77.3)	69.5 (72.1)	68.0 (68.6)
-2		151.0 (152.5)	115.0 (119.3)	103.0 (104.4)	93.5 (95.2)	87.0 (88.7)
-3				** (136.6)	117.5 (119.3)	106.0 (108.6)
-4					153.0 (153.0)	** (131.4)

60° From Normal

m	100	150	200	250	300	350
0	29.5 (30.0)	29.5 (30.0)	28.5 (30.0)	29.5 (30.0)	31.5 (30.0)	31.5 (30.0)
-1	108.5 (109.2)	85.0 (86.1)	73.5 (74.5)	66.5 (66.2)	61.5 (62.1)	57.5 (58.4)
-2	163.5 (*)	133.5 (136.8)	107.5 (109.3)	93.5 (95.2)	85.5 (86.1)	78.5 (79.6)
-3			159.5 (158.2)	124.5 (124.7)	108.5 (109.4)	97.5 (99.2)
-4					133.5 (136.9)	118.0 (120.2)
-5					161.5 (*)	** (147.5)

Spectra not shown at a given frequency are beyond cutoff
*Calculation indicates this spectra is beyond cutoff
**Transmitted pulse obscured by receiver

in a manner nearly identical to the reflection from an optical diffraction grating. This effect could make searching with SONAR for objects on a rippled ocean bottom extremely difficult.

The amplitudes of the various spectra were found to vary considerably with changes in frequency. At certain frequencies some spectra even disappeared completely. Measurements were made of the reflection coefficients for the spectral and first negative order reflections at an angle of incidence of 45 degrees. The results are shown as a function of frequency in figures 5.5 and 5.6.

These points were obtained by dividing the reflected pressure amplitude by the incident pressure amplitide as determined on a probe placed in the direct beam of the transmitter. The data was taken on two different sets of transducers which were calibrated separately. Agreement between the two sets of data was close. Also plotted are the theoretical reflection coefficients for Rayleigh's limiting case where the surface wavelength is much greater than the acoustic wavelength ($p \lessgtr k$). (This situation, utilized since no theory exists for $p \lesssim k$, is discussed in section three.)

This theory predicts that the reflection coefficient for the spectral reflection should be equal to $\alpha_r J_o$ (2hkcos θ) and that of the first order reflection $\alpha_r J_1$ (2hkcos θ). All quantities in the argument of the Bessel Functions have been previously determined. All that is needed is to determine the flat sand reflection coefficient, α_r, at the angle of incidence used to obtain the data.

The flat sand reflection coefficient, at an angle of incidence of 45 degrees, was measured for several frequencies and was found to vary

56

Figure 5.5 Reflection Coefficient for Rippled Sand

$\alpha_r^{I} = 0.42 \pm .03$

$\alpha_r^{II} = 0.29 \pm .05$

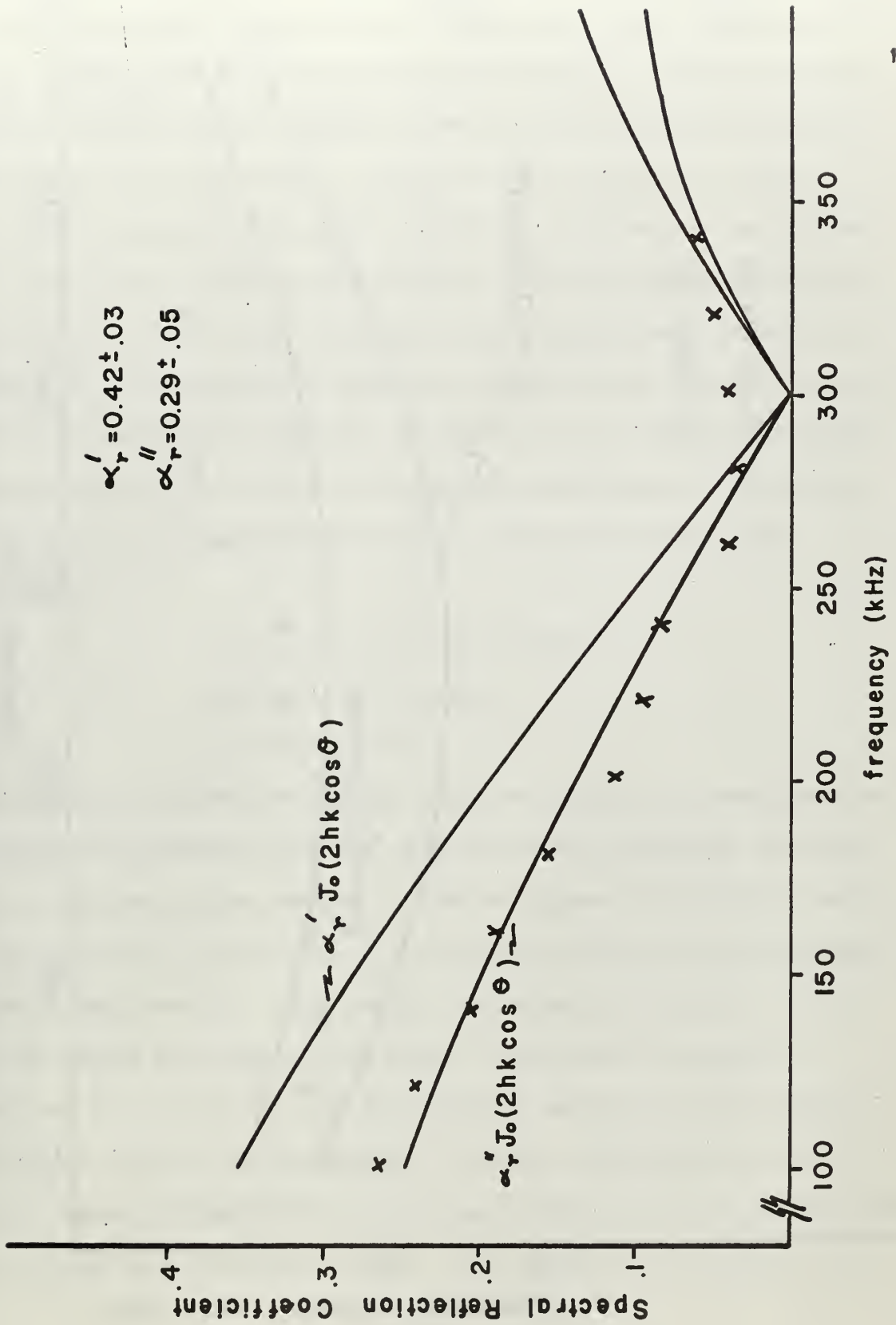$\alpha_r^{I} J_o(2hk\cos\theta)$

$\alpha_r^{II} J_o(2hk\cos\theta)$

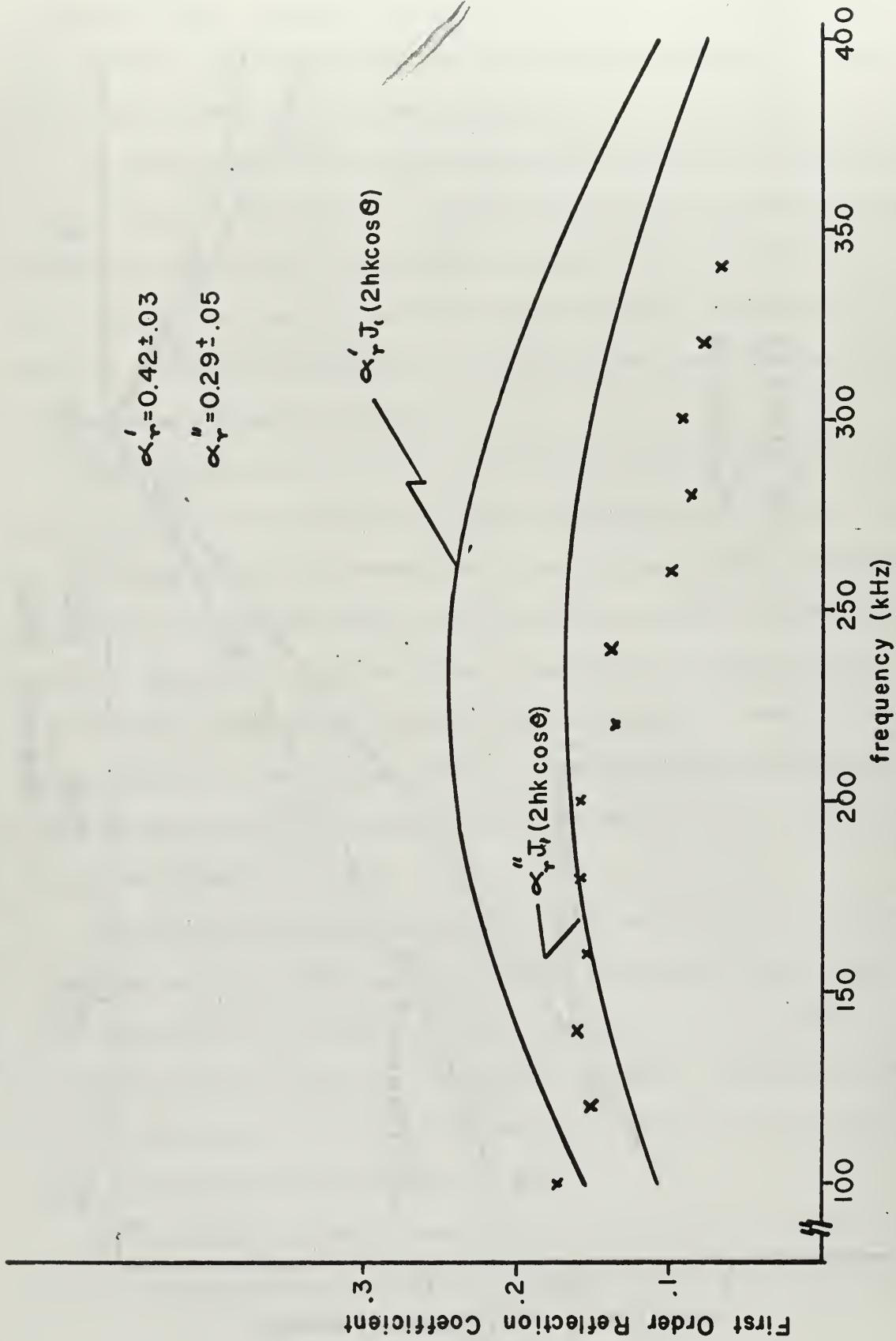frequency (kHz)

Spectral Reflection Coefficient

Figure 5.6 Reflection Coefficient for Rippled Sand

58

with frequency. The pattern of this variation changed when the transducers were changed although the mean remained the same. Therefore, it was considered that this variation was experimental. The flat sand reflection coefficient was obtained by determining the mean and standard deviation of the data points. This lead to a value of 0.29 $\pm$ .05.

This value of the reflection coefficient at 45 degrees is considerably smaller than would be predicted from information given earlier in this paper. In an attempt to resolve this anomaly it was decided to compute α_r using Rayleigh's reflection formula and the directly measured sand density and sound velocity, ρ_2 and C_2. C_2 was determined through a measurement of the critical angle, and ρ_2 was measured by weighing a small container of sand removed from the bottom of the tank. This resulted in:

$$C_2 = (1.65 \pm .04) \times 10^5 \text{ cm/sec}$$
$$\rho_2 = 1.91 \pm .05 \text{ gm/cm}^3$$
$$\alpha_r = 0.42 \pm .03$$

The difference between the two flat sand coefficients is larger than the estimated experimental error and, unfortunately, has not been resolved.

In the case of the spectral reflection (Figure 5.5) the first null point occurs at a position so as to indicate an 8% error in the argument of the Bessel Function. This could be explained by an error in measuring the ripple amplitude by this amount. The standard deviation of measuring the ripples was only four percent, assuming the cement cast accurately reflects the ripple shape. However, the measurements made directly from the rippled sand yielded approximately the same ripple height but did have an eight percent error. As a result, the position of the

59

first null can be said to agree with theory within the limit of maximum probable measurement error. Considering the amplitude, there is excellent agreement with theory if the directly measured α_r (0.29) is used. However, if the indirectly determined value of α_r is used, agreement is not good.

Turning to the first order reflection, (Figure 5.6) it can be seen that the amplitudes agree using the directly measured α_r except for a horizontal displacement of the theoretical curve of 80 to 90 kHz. The fact that reasonable agreement is once more obtained using the directly measured α_r supports the assumption that this is, in fact, the appropriate value for the flat sand reflection coefficient.

Given the assumption that the directly measured flat sand reflection coefficient is the proper one, the theory accurately predicts the reflection coefficient for spectral reflection from rippled sand. The agreement is not as good for the first order reflection. It seems that the difference in this latter case is caused, not by an error in α_r, but by an error in the theoretical expression for the argument of the Bessel Function or in lack of additional terms. Investigation of higher orders would be useful, but time did not permit.

6. Conclusions

Pulse techniques were developed and found suitable for use in a small reverberant tank within the frequency range 100-350 kHz. It was found feasible to construct a model of the ocean bottom, provided that the sand was boiled to remove entrapped air. This results in an interface which is a more realistic representation of the ocean bottom than is possible with either styrofoam or plaster. The sand surface could be mechanically shaped to represent the ripples which are frequently found on the ocean bottom.

The results show that scattering from a rippled sandwater interface occurs generally in the manner predicted by theory. The experimental diffraction angles agreed quite closely with theory, although the diffracted spectra nearest cutoff could not be predicted accurately. Often the highest order present was predicted to lie beyond cutoff.

The limiting case theory ($p \ll k$) accurately predicts the spectral reflection coefficient, but there is some error in the prediction of the first order reflection coefficient. Hence, it appears that Rayleigh's theory for scattering from a rippled surface into which sound can penetrate allows reasonably accurate prediction of the reflection coefficients. The degree of agreement is better than might be expected considering that the condition $p \ll k$ has been violated in this experiment.

More information can be gained by extension of the experiment to ripples of greater height, to a wider frequency range, and to an examination of the higher order reflections. It is hoped that such an effort will result in development of a more exact theory for predicting reflection from a rippled non-pressure release boundary.

61

7. Acknowledgements

8.   Bibliography

1.   Barnard, G. R., Bardin, J. L., and Hempkins, W. B.   Underwater
         Sound Reflection From Layered Media, J. Acoust. Soc. Am.
         36: 2119-2123 (1964).

2.   Department of the Army, Corps of Engineers, Wave-Generated Ripples
         in Nearshore Sands, Tech. Mem. 100   Oct. 1957.

3.   Eckart, C. The Scattering of Sound From The Sea Surface, J. Acoust.
         Soc. Am. Vol. 25: 566-570 (1953).

4.   Gallagher, J. J.   Some Design Considerations for a Marine Sediment
         In-Situ Measurement Probe----, USNUSL Report No. 617   March
         1965.

5.   Hamilton, E. L., Shumway, G., Menard, H. W., and Shipek, C. J.
         Acoustic and Other Physical Properties of Shallow-Water
         Sediments off San Diego, J. Acoust. Soc. Am. Vol. 28:
         1-15 1956.

6.   Heaps, H. S. Reflection of Plane Waves of Sound from a Sinusoidal
         Surface, J. Acoust. Soc. Am. Vol. 28:   815-818 (1957).

7.   Horton, C. W. Model Studies, Paper presented at 68th Meeting of
         the Acoust. Soc. Am. Oct. 21-24 1964 at Austin, Texas.
         Reprinted by AVCO Marine Electronics Office   Jan. 1965.

8.   Kinsler, L. F. and Fry, A. R. Fundamentals of Acoustics, 2nd
         Ed.   John Wiley & Sons, Inc. 1962.

9.   LaCasce, E. O. Jr. and Tamarkin, P. Underwater Sound Reflection
         from a Corrugated Surface, J. Appl. Phys. Vol. 27: 138-
         148 (1956).

10. Landau, L. D. and Lifshitz, E. M. Fluid Mechanics Pergamon Press,
         1959 pp 273-279.

11. Lord Rayleigh, Theory of Sound, Dover Publications, New York, 1945
         Vol. 2 (89-96).

12. Marsh, H. W. Exact Solution of Wave Scattering by Irregular
         Surfaces, J. Acoust. Soc. Am. Vol. 33, 330-333.

13. Menotti, F. R., Santaniello, S. R., and Schumacher, W. R.,
         Predicted Values of Bottom Reflectivity as a Function of
         Incident Angle, J. Acoust. Soc. Am. Vol. 38: 707-714.

14. Nolle, A. W., Hoyer, W. A., Mifsud, J. F., Runyan, W. R., and
     Ward, M. B. Acoustical Properties of Water-Filled Sands,
     J. Acoust. Soc. Am. Vol: 35-1394 (1963)

15. Officer, C. B. Introduction to the Theory of Sound Transmission,
     McGraw-Hill, 1958 (186-214).

16. Palatini, G. L. Electroacoustic Properties of Mylar Dielectric
     Underwater Sound Transducers, Thesis, U. S. Naval Postgraduate
     School, Monterey, California, May 1966.

17. Papadakis, E. P. Three Experiments on Diffraction from Periodic
     Surfaces, J. Acoust. Soc. Am. Vol: 38: 987-994 (1965).

18. Shipek, C. J. Photographic Survey of Sea Floor on Southwest Slope
     of Eniwetok Atoll, Geological Soc. of Am. Bulletin Vol. 73:
     805-812 (1962).

19. Shumway, G. Sound Speed and Absorption Studies of Marine Sedi-
     ments by a Resonance Method, Geophysics Vol. 25: 451-467,
     659-682 (1960).

20. Sptiznoggle, F. R. Scattering of a Plane Sound Wave by a Pressure-
     Release Sinusoid, Thesis, University of Texas Jan. 1965.

21. Uretsky, J. L. Reflection of a Plane Wave from a Sinusoidal
     Surface, J. Acoust. Soc, Am. 35: 1293-1294 (1963).

22. Yen, Nai-Chyuan and Middleton, F. H. Model Experiments on Under-
     water Sound Reflection From a Corrugated Boundary, University
     of Rhode Island, Tech. Rpt. 20 Oct. 1961, USNUOS, Newport,
     R. I. Contract N140 (122) 71793B.

INITIAL DISTRIBUTION LIST

No. Copies

1.   Defense Documentation Center   20
     Cameron Station
     Alexandria, Virginia 22314

2.   Library   2
     U. S. Naval Postgraduate School
     Monterey, California

3.   Bureau of Ships   1
     Navy Department
     Washington, D. C.   20360

4.   Office of Naval Research (Code 520)   1
     Washington, D. C.

5.   Professor James V. Sanders   5
     Department of Physics
     U. S. Naval Postgraduate School
     Monterey, California

6.   LCDR Philip Arcuni, USN   1
     % COMFAIRWGLANT
     Norfolk, Virginia

7.   Professor Alan B. Coppens   1
     Department of Physics
     U. S. Naval Postgraduate School
     Monterey, California

8.   Professor C. W. Horton   1
     Department of Physics
     University of Texas
     Austin, Texas
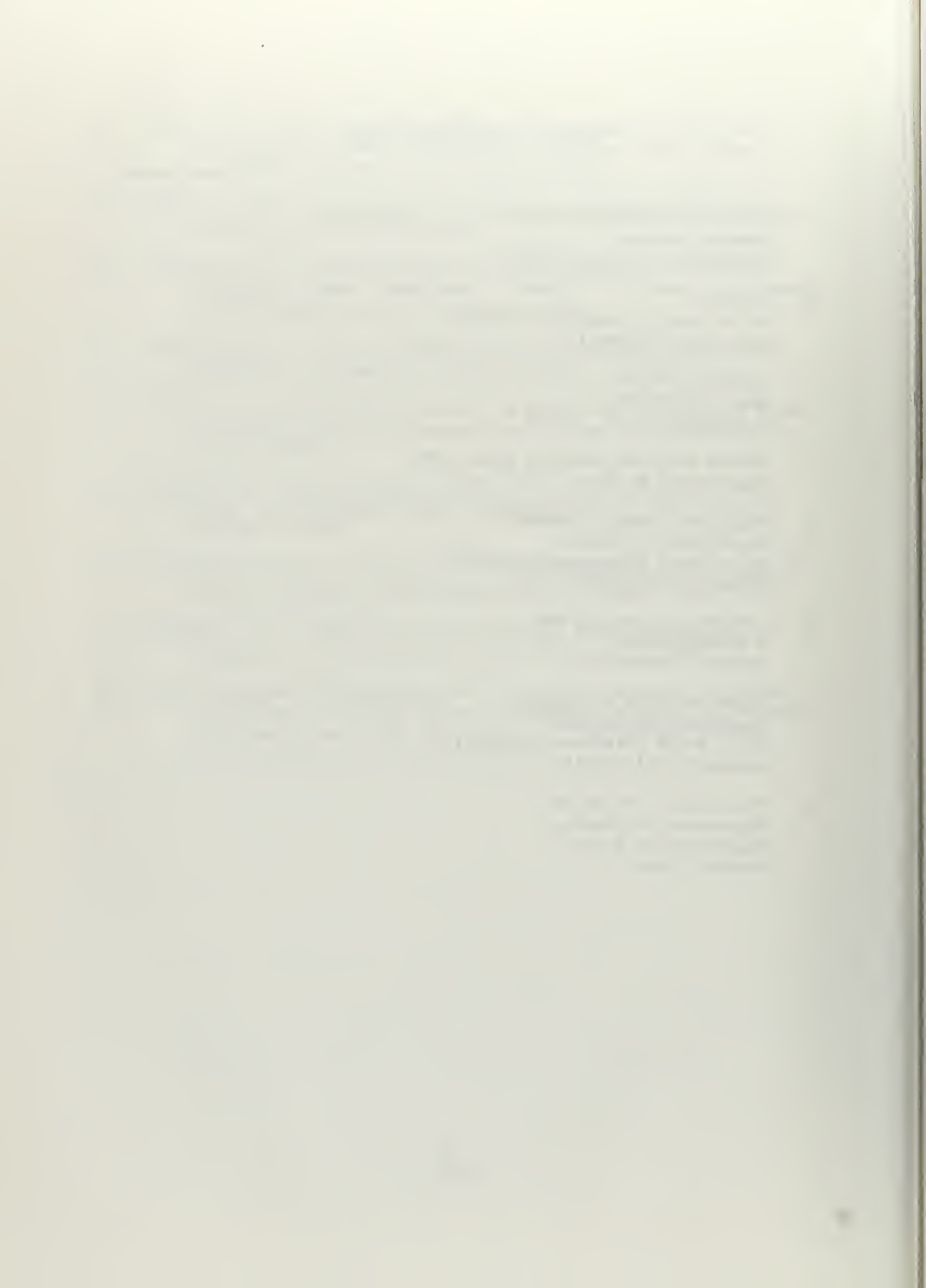
DOCUMENT CONTROL DATA - R&D		
(Security classification of title, body of abstract and indexing annotation must be entered when the overall report is classified)		

1. ORIGINATING ACTIVITY (Corporate author)	2a. REPORT SECURITY CLASSIFICATION
U. S. Naval Postgraduate School Monterey, California	Unclassified
	2b. GROUP N.A.

3. REPORT TITLE
A Model Study of Acoustic Reflection From a Rippled Water-Sand Interface

4. DESCRIPTIVE NOTES *(Type of report and inclusive dates)*
Thesis

5. AUTHOR(S) *(Last name, first name, initial)*

ARCUNI, Philip, LCDR, USN

6. REPORT DATE May 1966	7a. TOTAL NO. OF PAGES 65 6°	7b. NO. OF REFS 22
8a. CONTRACT OR GRANT NO. BuShips Allotment 172570	9a. ORIGINATOR'S REPORT NUMBER(S) N.A.	
b. PROJECT NO. Research Project RR 011-01-01		
c.	9b. OTHER REPORT NO(S) (Any other numbers that may be assigned this report) N.A.	
d.		

10. AVAILABILITY/LIMITATION NOTICES
~~Qualified requesters may obtain copies of this report from DDC~~ *Meuneken 10/9/69*

This document has been approved for public
~~release and sale; its distribution is unlimited.~~

11. SUPPLEMENTARY NOTES	12. SPONSORING MILITARY ACTIVITY
	Bureau of Ships Office of Naval Research Washington, D. C. Washington, D. C.

13. ABSTRACT

A model experiment was performed to measure acoustic reflection from a rippled sand surface using a pulse-echo system employing electrostatic transducers over the frequency range 100-350 kHz. The ripple wavelength of 1.23 cm was slightly greater than the longest acoustic wavelength and had an amplitude to wavelength ratio of 1/10. Boiling of the sand to remove entrapped air was essential before the scattering effects of the ripples could be observed. The angles of propagation of the scattered spectra are found to agree with the theoretical prediction within $\pm 2°$. The amplitudes of two orders of the scattered spectrum were measured at an incident angle of $45°$ and compared to the theory for the limiting condition where the ripple wavelength is very much larger than the acoustic wavelength. Agreement was excellent for the spectral reflection, but was not as good for the first order reflection.

DD FORM 1 JAN 64 **1473**

14. KEY WORDS	LINK A		LINK B		LINK C	
	ROLE	WT	ROLE	WT	ROLE	WT
Model Study						
Acoustic Reflection						
Ripples						
Sinusoidal Surface						
Sand						
Underwater Sound						

INSTRUCTIONS

1. ORIGINATING ACTIVITY: Enter the name and address of the contractor, subcontractor, grantee, Department of Defense activity or other organization (corporate author) issuing the report.

2a. REPORT SECURITY CLASSIFICATION: Enter the overall security classification of the report. Indicate whether "Restricted Data" is included. Marking is to be in accordance with appropriate security regulations.

2b. GROUP: Automatic downgrading is specified in DoD Directive 5200.10 and Armed Forces Industrial Manual. Enter the group number. Also, when applicable, show that optional markings have been used for Group 3 and Group 4 as authorized.

3. REPORT TITLE: Enter the complete report title in all capital letters. Titles in all cases should be unclassified. If a meaningful title cannot be selected without classification, show title classification in all capitals in parenthesis immediately following the title.

4. DESCRIPTIVE NOTES: If appropriate, enter the type of report, e.g., interim, progress, summary, annual, or final. Give the inclusive dates when a specific reporting period is covered.

5. AUTHOR(S): Enter the name(s) of author(s) as shown on or in the report. Enter last name, first name, middle initial. If military, show rank and branch of service. The name of the principal author is an absolute minimum requirement.

6. REPORT DATE: Enter the date of the report as day, month, year; or month, year. If more than one date appears on the report, use date of publication.

7a. TOTAL NUMBER OF PAGES: The total page count should follow normal pagination procedures, i.e., enter the number of pages containing information.

7b. NUMBER OF REFERENCES: Enter the total number of references cited in the report.

8a. CONTRACT OR GRANT NUMBER: If appropriate, enter the applicable number of the contract or grant under which the report was written.

8b, 8c, & 8d. PROJECT NUMBER: Enter the appropriate military department identification, such as project number, subproject number, system numbers, task number, etc.

9a. ORIGINATOR'S REPORT NUMBER(S): Enter the official report number by which the document will be identified and controlled by the originating activity. This number must be unique to this report.

9b. OTHER REPORT NUMBER(S): If the report has been assigned any other report numbers (either by the originator or by the sponsor), also enter this number(s).

10. AVAILABILITY/LIMITATION NOTICES: Enter any limitations on further dissemination of the report, other than those imposed by security classification, using standard statements such as:

(1) "Qualified requesters may obtain copies of this report from DDC."

(2) "Foreign announcement and dissemination of this report by DDC is not authorized."

(3) "U. S. Government agencies may obtain copies of this report directly from DDC. Other qualified DDC users shall request through

_____ ."

(4) "U. S. military agencies may obtain copies of this report directly from DDC. Other qualified users shall request through

_____ ."

(5) "All distribution of this report is controlled. Qualified DDC users shall request through

_____ ."

If the report has been furnished to the Office of Technical Services, Department of Commerce, for sale to the public, indicate this fact and enter the price, if known.

11. SUPPLEMENTARY NOTES: Use for additional explanatory notes.

12. SPONSORING MILITARY ACTIVITY: Enter the name of the departmental project office or laboratory sponsoring (paying for) the research and development. Include address.

13. ABSTRACT: Enter an abstract giving a brief and factual summary of the document indicative of the report, even though it may also appear elsewhere in the body of the technical report. If additional space is required, a continuation sheet shall be attached.

It is highly desirable that the abstract of classified reports be unclassified. Each paragraph of the abstract shall end with an indication of the military security classification of the information in the paragraph, represented as (TS), (S), (C), or (U).

There is no limitation on the length of the abstract. However, the suggested length is from 150 to 225 words.

14. KEY WORDS: Key words are technically meaningful terms or short phrases that characterize a report and may be used as index entries for cataloging the report. Key words must be selected so that no security classification is required. Identifiers, such as equipment model designation, trade name, military project code name, geographic location, may be used as key words but will be followed by an indication of technical context. The assignment of links, roles, and weights is optional.
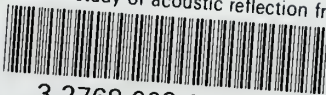
DD FORM 1473 (BACK)
1 JAN 64